AD-A061 928 NAVAL OCEAN SYSTEMS CENTER SAN DIEGO CA F/G 13/10
THE SIGNIFICANCE OF SEAMANSHIP AND POSITIVE SHIP CONTROL TECHNI--ETC(U)
JUL 78 J D KING
UNCLASSIFIED NOSC/TR-313 NL

| OF |
AD
A061928

END
3-79
DDC

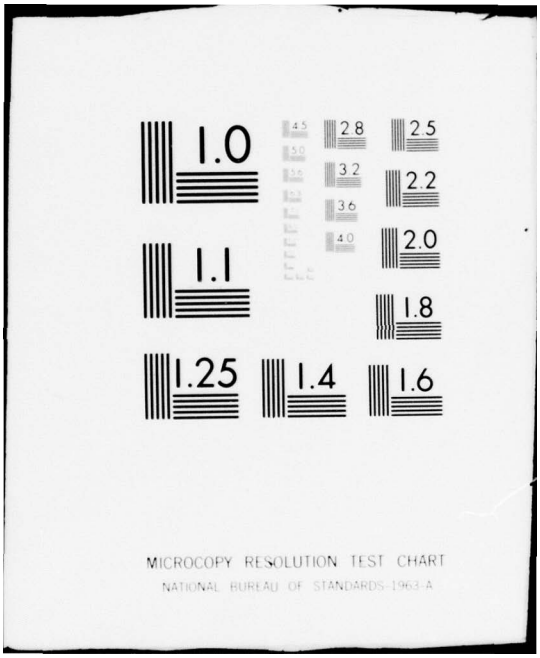
1.0
1.1
1.25
1.4
1.6
1.8
2.0
2.2
2.5
2.8
3.2
3.6
4.0
4.5
5.0
5.6
6.3
7.1
8.0
9.0
MICROCOPY RESOLUTION TEST CHART
NATIONAL BUREAU OF STANDARDS-1963-A

LEVEL

NOSC

NOSC TR 313

Technical Report 313

THE SIGNIFICANCE OF SEAMANSHIP AND POSITIVE SHIP CONTROL TECHNIQUES IN CONTROLLING ARRAY DYNAMICS

LCDR JD King

1 July 1978

Research and Development Report: Nov 1977 - May 1978

Prepared for
Long Range Acoustic Propagation Project
Naval Ocean Research and Development Activity

Approved for public release; distribution unlimited.

NAVAL OCEAN SYSTEMS CENTER
SAN DIEGO, CALIFORNIA 92152

NAVAL OCEAN SYSTEMS CENTER, SAN DIEGO, CA 92152

AN ACTIVITY OF THE NAVAL MATERIAL COMMAND

RR GAVAZZI, CAPT, USN
Commander

HL BLOOD
Technical Director

ADMINISTATIVE INFORMATION

This report was prepared under a subtask of work sponsored by Dr RD Gaul, Director of the Long Range Acoustic Propagation Program (LRAPP) at the Naval Ocean Research and Development Activity (Project No. 8119, Element 63795N). The effort described herein was performed on board the M/V SEISMIC EXPLORER and at the Naval Ocean Systems Center (NOSC) from November 1977 to July 1978.

The at-sea observations, theoretical studies, and computer modeling accomplished in support of this effort were integral to the Naval Ocean Systems Center LRAPP project under the co-ordinated task management of MR Akers, NOSC Code 714. Dr GE Martin and HS Aurand reviewed this report.

Released by
MR AKERS
NOSC LRAPP Program Manager

Under authority of
HA SCHENCK
Head, Undersea Surveillance Department

ACKNOWLEDGMENTS

Data-handling assistance and computer program development provided by Miss Ruth Creswell and statistics consultation services provided by Mr JD Pugh are gratefully acknowledged.

UNCLASSIFIED

SECURITY CLASSIFICATION OF THIS PAGE *(When Data Entered)*

REPORT DOCUMENTATION PAGE

READ INSTRUCTIONS BEFORE COMPLETING FORM

1. REPORT NUMBER: NOSC/TR-313
2. GOVT ACCESSION NO.:
3. RECIPIENT'S CATALOG NUMBER:

4. TITLE *(and Subtitle)*: THE SIGNIFICANCE OF SEAMANSHIP AND POSITIVE SHIP CONTROL TECHNIQUES IN CONTROLLING ARRAY DYNAMICS

5. TYPE OF REPORT & PERIOD COVERED: Research & Development, November 1977-May 1978

6. PERFORMING ORG. REPORT NUMBER:

7. AUTHOR(s): LCDR JD King

8. CONTRACT OR GRANT NUMBER(s):

9. PERFORMING ORGANIZATION NAME AND ADDRESS: Naval Oceans Systems Center, San Diego, California, 92152

10. PROGRAM ELEMENT, PROJECT, TASK AREA & WORK UNIT NUMBERS: Project No. 8119, Element 63795N

11. CONTROLLING OFFICE NAME AND ADDRESS: Naval Ocean Research and Development Activity, NSTL Station, Mississippi 39529

12. REPORT DATE: 1 July 1978

13. NUMBER OF PAGES: 61

14. MONITORING AGENCY NAME & ADDRESS *(if different from Controlling Office)*:

15. SECURITY CLASS. *(of this report)*: Unclassified

15a. DECLASSIFICATION/DOWNGRADING SCHEDULE:

16. DISTRIBUTION STATEMENT *(of this Report)*

Approved for public release; distribution unlimited

65 pp. Technical rept. Nov 77-May 78

17. DISTRIBUTION STATEMENT *(of the abstract entered in Block 20, if different from Report)*

18. SUPPLEMENTARY NOTES

19. KEY WORDS *(Continue on reverse side if necessary and identify by block number)*

towed arrays
linear regression analysis
dynamic modeling

20. ABSTRACT *(Continue on reverse side if necessary and identify by block number)*

The application of positive ship control techniques and the utilization of prudent seamanship are paramount in controlling the dynamics of long towed arrays. To this end, the maintenance of constant ship speed, and hence array speed, is fundamental in minimizing array deformation. Unfortunately, this heavily sea-state-dependent variable is virtually uncontrollable when "conventional" converted oil drilling support vessels are employed as towing vessels. For many cases, linear regression analysis appears to adequately describe vertical array deformation. The need is clear for increased *in situ* array monitoring to provide a more thorough understanding of the parameters directly affecting array dynamics.

DD FORM 1 JAN 73 1473 EDITION OF 1 NOV 65 IS OBSOLETE
S/N 0102-LF-014-6601

UNCLASSIFIED

SECURITY CLASSIFICATION OF THIS PAGE *(When Data Entered)*

393 159

CONTENTS

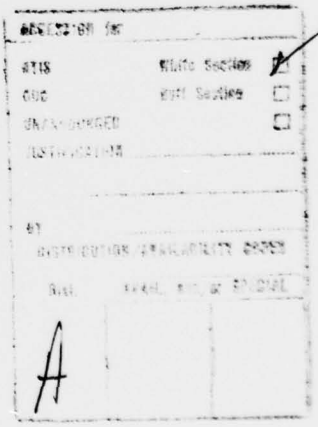

ILLUSTRATIONS

TABLES

INTRODUCTION

BACKGROUND

An inherent problem with long-line towed arrays has been the nearly continuous departure of the array shape from a completely horizontal and vertical neutral state. Many investigators, in order to understand the difficult problem of array dynamics, have developed computerized models of varying complexity (Refs. 1-5). Many of the models developed have assumed a number of ideal conditions to keep the model within workable and economic bounds. Because of these restraints, the outputs of the models are not always representative of the real world. The intent of this paper, then, is threefold: (1) to analyze in detail the approximately 165 hours of non-acoustic sensor data taken with the Large Aperture Marine Basic Data Array (LAMBDA); (2) to study the role of seamanship and ship handling and their effects on array dynamics; and (3) to make available to the towed-array community a set of validated non-acoustic data to be used for model validation, towed-array simulator development, and for planning future sea-going endeavors.

SCOPE OF STUDY

This effort is limited to the analysis of non-acoustic sensor data taken with the LAMBDA array deployed aboard the M/V SEISMIC EXPLORER during a specific exercise conducted in the Western Pacific Ocean in late 1977. Data, recorded automatically on the Non-acoustic Data System (NADS), is convolved with data such as this author's personal observation of ship-handling evolutions. Statistical and graphical analyses are applied whenever possible during this study in order to comprehend further the elusive problem of array dynamics. In the interest of ensuring timely and extensive distribution of this study, no attempt is made at this juncture to compare the information within this report with previously developed array dynamics models and theories. The author recognizes that such an effort would be a logical follow-on and should be accomplished to advance the state-of-the-art of the long-line towed array dynamics problem.

PROCEDURE

DATA RECORDING EQUIPMENT

A majority of the data utilized in this study was extracted from computer printouts of the NADS. A sample printout is shown in Fig. 1.

NADS READOUT RDG # 2345 TIME: 01:23:56

SLAT	SLNG	STIME	DLAT	DLNG	DTIME
89:23.0 N	123:06.1 W	01:06:16	89:23.0 N	123:06.6 W	01:20:15

HS	HG	CN	SN	SS	DEV
45.0	45.1	46.0	14.1	12.4	0.0

H1	D1	T1	D2	T2	D3	T3	H3	D4	T4	H5	D5	T5
45.1	0.0	????	0.0	????	0.0	????	45.2	0.0	????	45.0	0.0	????

PT	PD	SG	AT	FT	PF	TS	WS	WDA	WSN	WD	WSA	XBT
????	0.0	48	2	3	0	????	24.0	0.1	0.1	225.0	10.0	????

MNEMONIC	MEANING
RDG#	NADS reading no.
TIME	Time of reading
SLAT	SATNAV latitude
SLNG	SATNAV longitude
STIME	Time of last SATNAV fix
DLAT	Dead reckoning latitude
DLNG	Dead reckoning longitude
DTIME	Time of last dead reckoning fix
HS	Heading via SATNAV unit
HG	Heading via gyro
CN	Ship's course via SATNAV unit
SN	Ship's speed via SATNAV unit
SS	Ship's speed via knotmeter
DEV	Deviation between gyro and magnetic compass (not connected)
H1,H3,H5	Array heading sensors, 1, 3, and 5
D1,D2,D3,D4,D5	Array depth sensors 1, 2, 3, 4, and 5
T1,T2,T3,T4,T5	Array temperature sensors 1, 2, 3, 4, and 5
PT	Precision tension (array)
PD	Precision depth (array)
SG	SCU gain
AT	Array type
FT	Filter type
PF	Power fail (not connected)
WS	Wind speed (relative)
WDA	Wind direction (absolute)
WSN	Wind speed (normal)
WD	Wind direction (relative)
WSA	Wind speed (absolute)
XBT	XBT

Figure 1. Sample NADS readout.

Types and location of non-acoustic sensors used in this study are discussed below:

1. *Depth (D), temperature (T),* and *heading (H), sensors* and sensor numbers and locations within the array are shown in Fig. 2. The following sensors were inoperative during Cruise 5: temperature sensor #4 and depth sensors #1 and #4. Further, heading sensor #5 was inoperative during the first portion of the cruise.

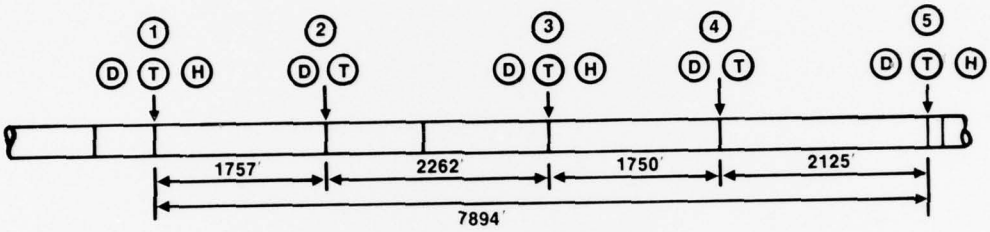

Figure 2. Sensor location.

2. *Ship's Speed (SS) – Knot Meter* – was of a propeller-driven variety mounted approximately centerline, amidships on the underwater hull of the SEISMIC EXPLORER.

3. *Ship's Heading (HS)* – was taken from a continual update via the SATNAV unit (an integrated satellite-doppler-sonar unit with a listed position accuracy of 200–600 ft).

4. *Ship's Position (SLAT, SLNG)* – was determined utilizing an integrated navigational system consisting of a Magnavox MX-702 satellite receiver, Hewlett-Packard 2115 digital computer, Marquardt MRQ-2015A doppler sonar, and a NUS TR3 Sperry gyro compass.

5. *Wind Speed and Direction Indicators (WS and WD)* – relative wind was measured with a propeller-type anemometer mounted on the ship's main mast. True wind was subsequently calculated by knowing the ship's course and speed and using a maneuvering board for solving the resulting vector triangle.

DATA LOGS

ARRAY SENSOR DATA LOG

The data inputs discussed above were extracted from the NADS printout and recorded in the more readily usable format of Fig. 3. Information displayed in Fig. 3 is essentially self-explanatory. Sea state determinations were based on the Beaufort scale, while average readings in the heading block were filled in after the ship had transitted an entire course leg; i.e., Station(s) TE-L26 represents a leg in this case.

Station(s) TE-L26, Array depth (Ave) ② 355 (m) ③ 400 (m) ⑤ 418 (m) Scope of wire 1650 ft, XBT no(s) 64

Lat. _____(start), Long. _____(start), True wind dir'n 020°T, Spd 12 kt

Lat. _____(stop), Long. _____(stop), Sea state 3

Ship's ave spd over grnd 2.12 kt, Ship's ave spd thru water 2.34 kt

Ship's cse good ovr grnd 020°T, Ship's ave head 028°T, Heading sen's ave hd ① 034°T ③ 036°T ⑤ 033°T

Time (Z)	Speed kt mtr	Ship's Cse (°T)	Sensor Readings									
			Heading (mag)			Temperature (°C)				Depth (m)		
			①	③	⑤	①	②	③	⑤	②	③	⑤
7 Dec 1439	2.2	037	040	?	001	11.4	10.3	?	8.8	303	?	367
1449	2.5	031	038	?	009	11.4	10.4	?	8.9	320	?	369
1509	2.5	029	033	?	007	11.4	10.4	?	9.1	327	?	367
1527	2.5	034	032	?	001	11.3	10.3	?	9.1	334	?	380
1547	2.3	031	036	?	029	11.2	10.2	?	9.1	328	?	389
1559	2.3	033	035	?	025	11.2	10.2	?	9.0	335	?	388
1619	2.3	027	039	037	032	11.1	10.1	?	8.9	334	?	394
1639	2.3	033	035	?	034	11.0	10.0	?	8.8	340	?	399
1659	2.4	025	041	036	034	10.8	9.7	?	8.7	345	?	414
1719	2.2	022	039	037	039	10.8	9.6	9.1	8.6	347	365	421
1739	2.3	027	035	041	041	10.5	9.4	9.1	8.5	366	383	424
1759	2.1	029	029	035	043	10.2	9.3	?	8.3	369	?	427
1819	2.4	022	035	034	037	10.0	9.1	8.8	8.2	367	393	444
1839	2.4	028	031	036	036	9.8	9.0	8.7	8.2	385	401	447
1859	2.3	027	033	036	036	9.7	8.8	8.5	8.1	385	407	457
1919	2.2	027	034	037	036	9.6	8.7	8.4	8.0	393	412	457
1939	2.5	024	028	037	038	9.6	8.7	8.3	7.9	389	413	472
1959	2.4	025	023	034	033	9.6	8.7	8.3	7.8	384	409	466

Figure 3. Sample array sensor data log.

NAVIGATIONAL PLOT

The ship's course made good over ground was determined by plotting recorded ship's positions on a standard H.O. latitude-corrected plotting sheet as shown in Fig. 4. For reconstruction purposes, the proposed track, in accordance with the Exercise Plan, was also plotted. Note that the normal 1-nm graduations have been omitted from this figure to facilitate visual presentation.

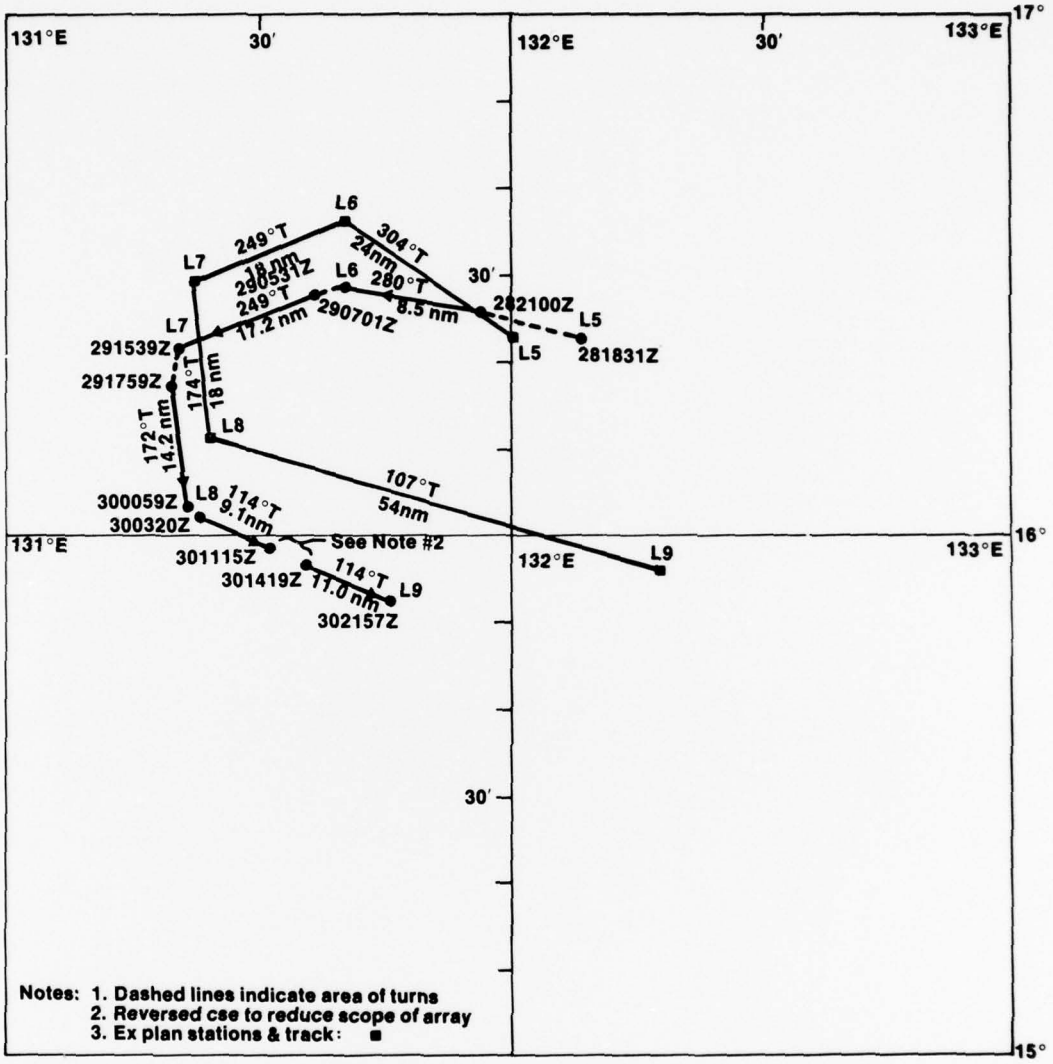

Figure 4. Sample navigational plot.

ARRAY SHIP HANDLING MANEUVERS LOG

Figure 5 represents a sample ship-handling log. The intent of this effort was to document all ship-handling evolutions during the times of major course changes. The compass rose in the upper right hand corner of the log displays the ship's initial and final course vectors (shown emerging from the center of the rose), wind speed and direction vector and sea and swell celerity and direction vector.

Station no I 28 True wind dir'n 060°T, Speed 14 kt
Initial cse 060°T Seas — dir'n 050°T, Heigh 6-8 ft
Final cse 138°T Swell — dir'n —°T, Height —ft
△ cse change 78° Sea state 3
Time start cse chg 0100 Z (11 Dec)
Time compl cse chg 0121 Z
Engine(s) on line Stbd (180 shaft rpm, 2.5 ktmtr)
Engine mode of op Normal
Ave D.A.D. kt mtk spd 2.43 kt (See NADS)
Rudder ∢ S, time, & ship handling remarks

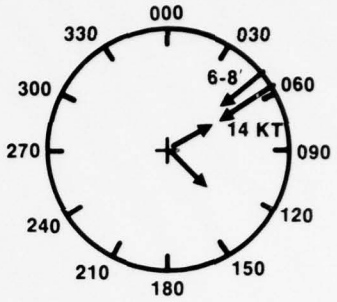

1. **0100 Rt 10° rudder, manual control**
2. **0105 Rudder amidships, head 142°**
3. **0107 Rt 5° rudder, head 134°**
4. **0107 Rudder amidships**
5. **0108 Rt 5° rudder, head 129°, shift to autopilot**
6. **0121 Steady 138°T to make 160°T good, 3.0 kt per ktmtr**
7. **0124 Reduce shaft rpm to ~165 (2.3 kt per ktmtr)**
8.
9.
10.
11.
12.

Note: Ship's speed was increased from 2.0 kt (ktmtr) to 2.5 kt (ktmtr) 15 min prior to turn and held 30 min into the turn in an effort to keep the array from sinking.

Figure 5. Sample array ship-handling maneuvers log.

DATA ANALYSIS TECHNIQUE

TIME SERIES PLOTS

The sensor data tabulated in Fig. 3 was keypunched and entered into a UNIVAC 1110 data storage bank. In order to analyze carefully the shape of the array in the time domain, a series of plots of array heading and array depth (vertical deplacement) versus time were generated. Figure 6 represents a sample of this data. The sensors are identified by their respective number, while c denotes the ship's course and v represents the ship's speed as measured by the installed knotmeter (kt mtr). Areas of discontinuous data represent times in which one or more of the sensors were inoperative or considered to be unreliable in the light of post analysis. Data sampling times varied from a 10- to 20-min interval for normal leg (station-to-station) transits to a 2-min sampling interval during the time the ship and the array were determined to be in a state of flux, i.e., major course and/or speed change evolutions. The time series plots served as the foundation for a large portion of the analyses that follow. A complete record of the time series plots may be found in the Appendix.

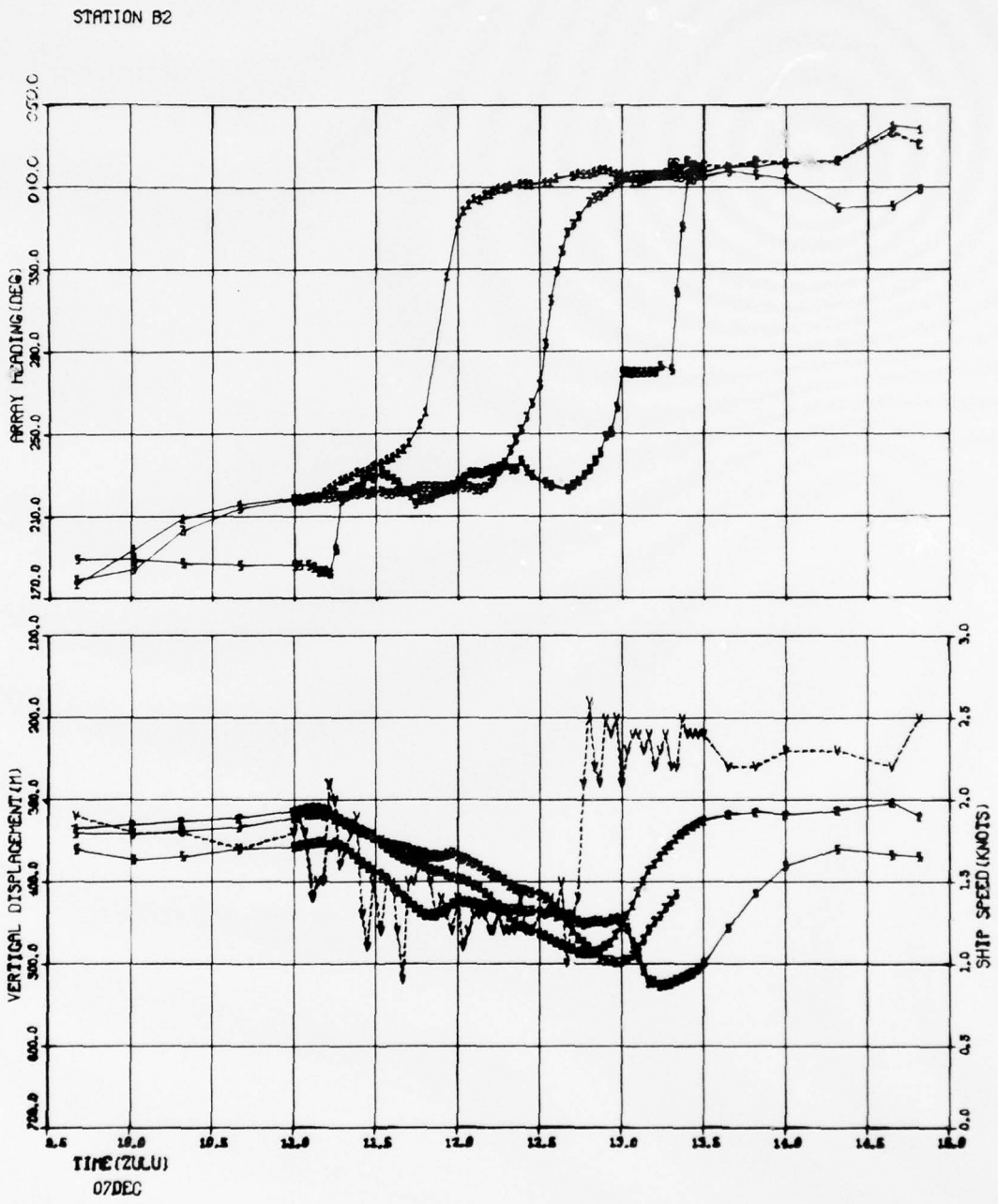

Figure 6. Sample time series plot.

REGRESSION ANALYSIS

LEAST SQUARE REGRESSION ANALYSIS

Visual inspection of the time series plots suggests that the argument of linearity may be applicable to describe the shape of the array in the vertical dimension for the normal transiting situation. Conversely, the linearity argument does not appear to be a viable solution to describe array behavior in the horizontal plane. To test the hypothesis of linearity, least square regression analysis was employed. Assume a linear relationship of the general form

$$Y = mX + b \tag{1}$$

where the defining coefficients m and b are given by

$$m = \frac{\sum_{i=1}^{n} (X_i - \overline{X})(Y_i - \overline{Y})}{\sum_{i=1}^{n} (X_i - \overline{X})^2}, \quad b = \overline{Y} - m\overline{X} \tag{2}$$

where

$$\overline{Y} = \frac{\sum_{i=1}^{n} Y_i}{n} \quad \text{and} \quad \overline{X} = \frac{\sum_{i=1}^{n} X_i}{n}$$

and

n = number of samples

substituting Eq. (2) into Eq. (1) yields the estimated regression equation

$$Y = \overline{Y} + m(X - \overline{X}) \tag{3}$$

COEFFICIENT OF DETERMINATION

In data analysis, it is often useful to ascertain what portion of the total variation is explained or unexplained, i.e., whether the deviations have a definite pattern (explained) or behave in a random or unpredictable manner (unexplained). Mathematically, the total variation is given by

$$\Sigma(Y-\overline{Y})^2 = \Sigma(Y-Y_{est})^2 + \Sigma(Y_{est} + \overline{Y})^2 \tag{4}$$

where Y_{est} = value of Y for given values of X as estimated from Eq. (1).

The first term on the right of Eq. (4) is the unexplained variation, while the second term is called the explained variation. The ratio of the explained variation to the total variation is known as the coefficient of determination, or

$$r^2 = \frac{\Sigma(Y_{est} - \overline{Y})^2}{\Sigma(Y - \overline{Y})^2} \tag{5}$$

where r^2 is a measure of the proportion of total variation about the mean $\overline{Y}$ explained by the linear regression.

SIGNIFICANCE OF THE LINEAR REGRESSION MODEL

Significance of linear regression may be tested by examining the slope m. The standard error of m is the square root of the variance, or

$$\text{s.e.}(m) = \frac{\sigma}{\left\{\Sigma(X_i - \overline{X})^2\right\}^{1/2}}$$

where σ = standard deviation. But since σ is unknown, the estimate s is used in its place, assuming the linear regression model is correct, and the estimated standard error of m is given by

$$\text{est s.e.}(m) = \frac{s}{\left\{\Sigma(X_i - \overline{X})^2\right\}^{1/2}} \tag{6}$$

Further, if we assume that the variations of the observations about the line are normal, it can be shown that we can assign $100(1-\alpha)\%$ confidence limits for m by calculating

$$m \pm t(n-2, 1-1/2\alpha)(\text{est s.e.}(m)) \tag{7}$$

where $t(n-2, 1-1/2\alpha)$ is the $(1-1/2\alpha)$ percentage point of a t-distribution, with $(n-2)$ degrees of freedom (the number of degrees of freedom on which the estimate s^2 is based). The slope m, and, hence, linear regression, is considered to be significant if its calculated value falls within the confidence level limits for a specified α.

F-TEST FOR GOODNESS-OF-FIT

A second check of the linear regression model takes the form of the F-test for goodness-of-fit. In other words, how well does the generated linear regression line fit the data? To comprehend the importance of testing a linear regression model for both significance of regression and goodness-of-fit, examine the typical straight-line regression arguments summarized in Fig. 7. The ϵ term of the regression model of Fig. 7 represents the increment

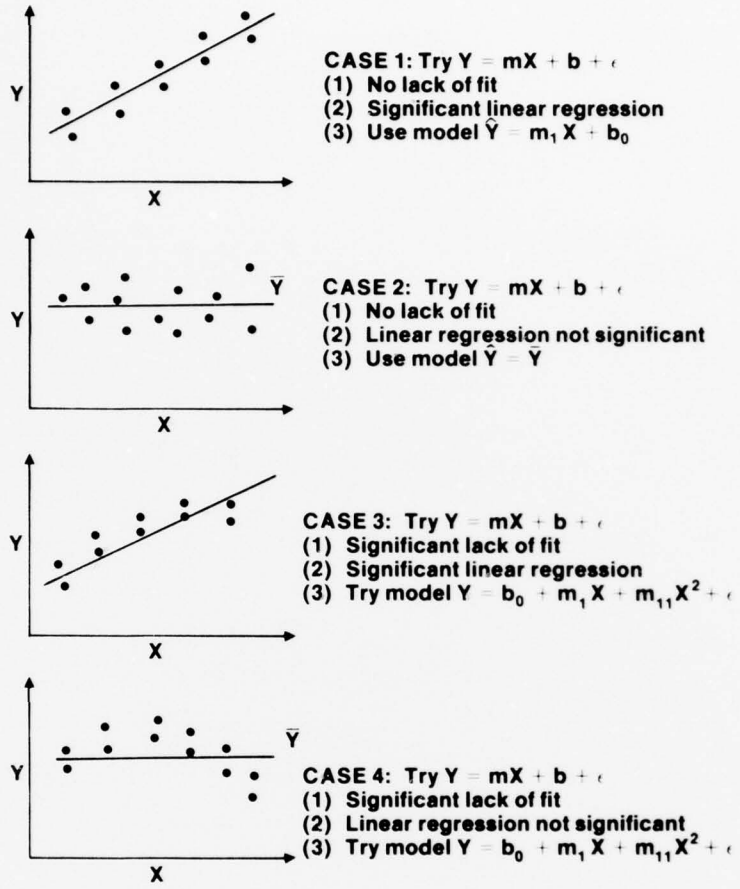

Figure 7. Typical straight-line regression arguments.

by which any individual Y may fall off the regression line. Referring to Fig. 7, it can be seen that it is entirely possible to have a model with significant linear regression and significant lack of fit or vice versa. Hence, the need for the goodness-of-fit test. The governing condition for application of this test is that replication of one of the variables exists. In this case the X variable, representing the horizontal location of a given array sensor, is fixed or controlled, while Y is the random variable and represents the vertical position in the water column of the sensor as a function of time.

Since Y is a random variable, any function of Y is also a random variable. Two particular functions are MS_L, the mean square due to pure error, and s_e^2, the mean square due to lack of fit. A statistical theorem (Ref. 6) tells us that these independent variables are related by:

$$F = \frac{MS_L}{s_e^2} \tag{8}$$

The task, then, is to compare a given F-ratio with the $100(1-\alpha)\%$ of the tabulated $F(1, n-2)$ distribution. The F-ratio is considered to be *significant* if $F > 100(1-\alpha)$ and the model subsequently rejected for lack of fit. Conversely, if $F < 100(1-\alpha)$, the F-ratio is *not significant* and we have no grounds to reject the model for lack of fit. In fact, if the F-ratio is not significant then both the pure error and the lack of fit terms of Eq. (8) can be used as estimates of the variance σ^2. Note: It can be shown (Refs. 6, 7), that the F-distribution is directly related to the t-distribution by $F = t^2$. Further, both the F- and t-distributions are derived from the Chi-Square distribution.

ENVIRONMENTAL EFFECTS

To analyze objectively wind and sea swell effects on ship and, hence, array motion, the convention illustrated in Fig. 8 was adopted. The aspect-determination descriptors are traditional, and for the cases of wind and seas coming from different sectors, the term "mixed" is assigned. The force scale is based loosely on the Beaufort scale.

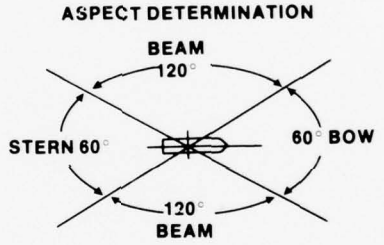

FORCE-SCALE

WIND (kts)	SEAS (ft)	DESCRIPTOR
5-10	2-4	LIGHT
10-15	4-6	GENTLE
15-20	6-8	MODERATE
20-25	8-10	STRONG
25-30	10-12	SEVERE

Figure 8. Wind and sea effect determinants.

DATA ANALYSIS RESULTS

LINEAR REGRESSION ANALYSIS

The linear regression model and goodness-of-fit techniques discussed earlier were applied to discrete time sets identified from the time series plots of the Appendix. Time sets were first identified by visual inspection techniques. Obviously, times of major array perturbation, i.e., ship/array turns, were excluded from this type of analysis and are addressed in a separate section of this report. Figure 9 illustrates an example of a computer fit of the linear regression model to a representative set of data for both the horizontal and vertical planes. Note that the correlation coefficient, r, is calculated in this case. However,

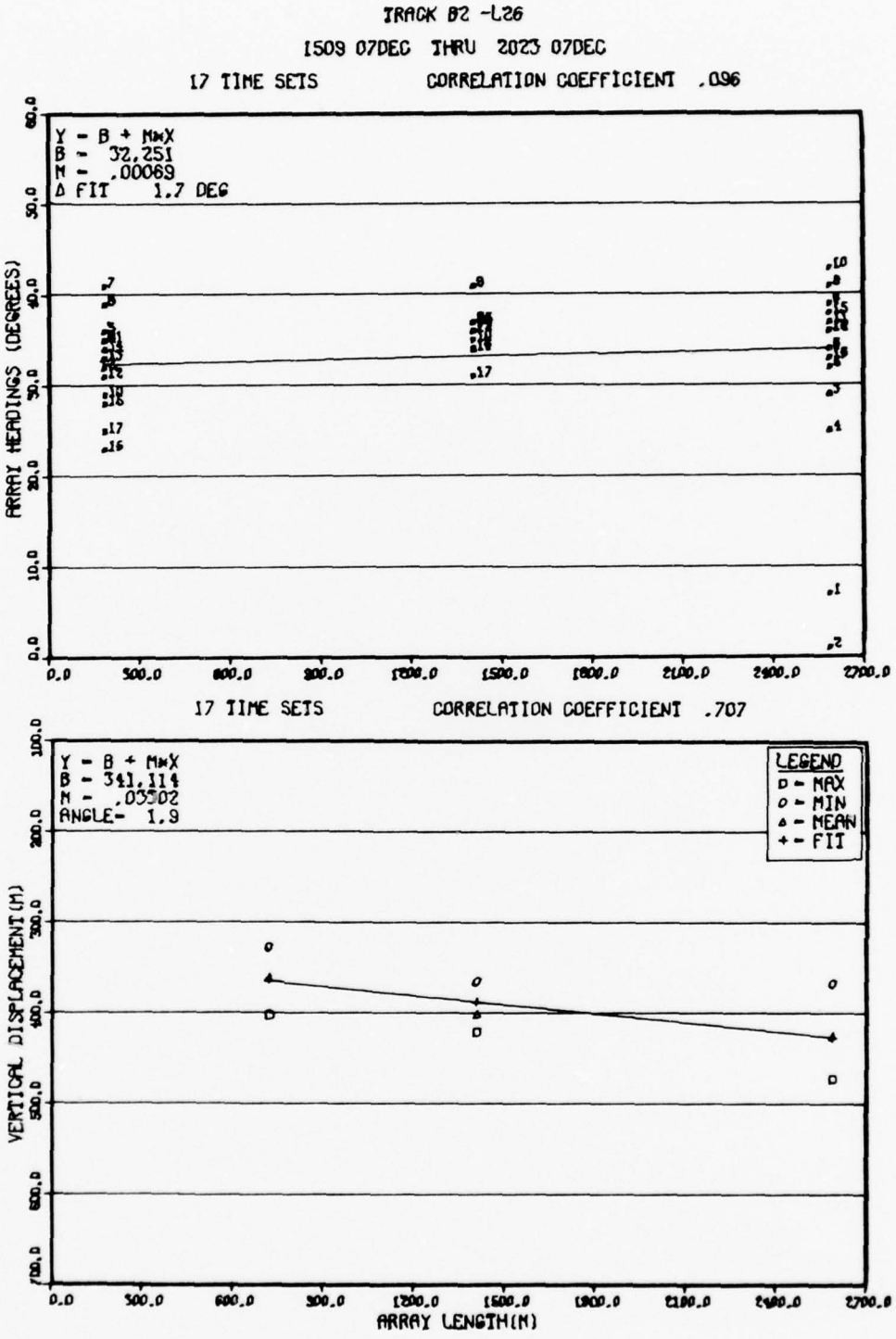

Figure 9. Sample linear regression model fit.

for the analysis that follows the coefficient of determination, r^2, was utilized as a more realistic determinant of explained variation. A separate program was next employed to test the linear regression model for significance of regression and goodness-of-fit. Tables 1 and 2 summarize the analysis of the linear regression model for the vertical and horizontal profiles, respectively. In applying the F- and t-distributions, the 0.95 interval was chosen as a baseline for the statistical analysis. That is, a one-in-twenty chance of the model not being representative of the data was considered a reasonable, and generally acceptable, risk.

The statistical results shown in Tables 1 and 2 are, for the most part, intuitive. For the vertical profile, the linear regression model was acceptable for 93%(27/29) of the cases. Conversely, the rejection argument dominated the horizontal profile statistics with a figure of 87%(14/16 cases). Recall that the smaller number of cases in the horizontal profile is due to the fact that heading sensor #5 was inoperative during the first part of the exercise. Further, the applicability of linear regression analysis is dependent on at least three x-component data points, two to define the linear relationship and one (degree of freedom) to test the generated model.

Table 1. Vertical profile regression statistics.

Track	Coef of Determ, r^2	Slope, b_1	0.95 Conf of $b_1(\pm)$	Deg of frd, f	F-stat	0.95F-Dist	Accept Model	Reject Model	
								Lack of Fit	Lack of Lin Reg
A1-A2(1)	0.86	0.0442	0.0021	24	0.00010	4.26	X		
A1-A2(2)	0.49	0.0079	0.0026	38	0.00018	4.10	X		
A1-A2(3)	0.13	0.0093	0.0099	30	8.65	4.17		X	X
A1-A2(T)	0.04	0.0119	0.0059	95	0.00002	3.92	X		
A2-L5(1)	0.96	0.0270	0.0024	22	0.43	4.30	X		
A2-L5(2)	0.92	0.0321	0.0033	27	0.017	4.21	X		
A2-L5(T)	0.74	0.0294	0.0022	53	0.016	4.02	X		
L5-L6	0.71	0.0815	0.0134	58	0.012	4.00	X		
L6-L7	0.76	0.0596	0.0069	72	0.0028	3.98	X		
L7-L8	0.53	0.0608	0.0143	60	0.030	4.00	X		
L8-L9(1)	0.90	0.1042	0.0095	46	0.0053	4.05	X		
L8-L9(2)	0.92	0.0826	0.0038	137	0.81	3.92	X		
B1-B2	0.85	0.0216	0.0036	26	4.06	4.23	X		
B2-L26	0.56	0.0347	0.0090	37	1.36	4.10	X		
L26-L27(1)	0.59	0.0393	0.0102	40	0.078	4.08	X		
L26-L27(2)	0.48	0.0467	0.0452	113	0.0077	3.92	X		
L26-L27(3)	0.83	0.0223	0.0035	29	0.0048	4.18	X		
L26-L27(T)	0.26	0.0394	0.0095	185	1.26	3.92	X		
L27-L28(1)	0.88	0.0743	0.0168	43	0.11	4.07	X		
L27-L28(2)	0.79	0.0573	0.0075	59	0.51	4.00	X		
L27-L28(3)	0.83	0.0346	0.0066	21	1.04	4.32	X		
L27-L28(4)	0.81	0.0640	0.0093	45	0.15	4.06	X		
L27-L28(5)	0.81	0.0449	0.0084	26	0.32	4.23	X		
L27-L28(6)	0.94	0.0690	0.0088	14	0.21	4.60	X		
L27-L28(7)	0.77	0.0536	0.0106	30	0.19	4.17	X		
L27-L28(8)	0.90	0.0571	0.0023	46	0.27	4.05	X		
L27-L28(T)	0.42	0.0568	0.0075	297	2.63	3.92	X		
L28-L29	0.55	0.0296	0.0112	22	0.00001	4.30	X		
L29-L30	0.48	0.0436	0.0155	56	7.73	4.01		X	

Table 2. Horizontal profile regression statistics.

Track	Coef of Determ, r^2	Slope, b_1	0.95 Conf of b_1 (±)	Deg of frd, f	F-stat	0.95F-Dist	Accept Model	Reject Model: Lack of Fit	Reject Model: Lack of Lin Reg
B1-B2	0.53	0.0046	0.0176	17	4.56	4.45		X	X
B2-L26	0.19	0.0018	0.0013	32	0.81	4.15	X		
L26-L27(1)	0.14	0.0014	0.0013	48	17.04	4.05		X	
L26-L27(2)	0.25	0.0025	0.0009	98	5.87	3.93		X	
L26-L27(3)	0.05	0.0010	0.0014	31	0.09	4.16			X
L26-L27(T)	0.05	0.0011	0.0041	183	3.23	3.92			X
L27-L28(1)	0.04	0.0016	0.0028	33	2.93	4.15			X
L27-L28(2)	0.44	0.0026	0.0007	58	5.84	4.00		X	
L27-L28(3)	0.42	0.0042	0.0197	24	0.60	4.26			X
L27-L28(4)	0.01	0.0002	0.0028	36	1.00	4.12			X
L27-L28(5)	0.09	0.0024	0.0025	31	0.07	4.16			X
L27-L28(6)	0.01	0.0005	0.0021	13	1.66	4.67			X
L27-L28(7)	0.31	0.0033	0.0026	25	24.58	4.24		X	
L27-L28(8)	0.02	0.0010	0.0021	45	0.14	4.06			X
L27-L28(T)	0.01	0.0009	0.0012	286	0.002	3.92			X
L28-L29	0.07	-	-	-	-	-			
L29-L30	0.33	0.0066	0.0024	58	0.22	4.00	X		

WIND AND SEA EFFECTS

Wind and sea/swell conditions have generally adversely affected ship-handling evolutions since man first began to sail. In the case of slow ship speeds and keel-less, U-shaped hull configurations, the adverse effect is even more pronounced. Throughout the cruise tow speeds of less than 3 knots were experienced, which often added to the burden of maintaining positive ship control, especially with the ship heading into the wind and seas. Compounding the ship-handling problem was SEISMIC EXPLORER's tendency to react like a cork when exposed to long-period swells, which were evidenced a majority of the time due to the presence of typhoon Lucy in the Western Pacific Basin. The sluggish ship handling responsiveness and cork-like effects of the SEISMIC EXPLORER are caused by a combination of inherent ship design features, the most prominent being the U-shaped, keel-less hull configuration, and the ship's relatively shallow draft (generally between 9 and 11 ft).

Wind and sea effects are summarized in Table 3, using the convention of Fig. 8 for defining aspect and force descriptors. The (½) entry in the sixth column of the table reflects those cases in which heading sensor #5 was inoperative. Thus, for these cases, the average deflection is taken over only about one-half of the array length. The critical parameter to be observed in this tabulation is the average array deflection entry (Column 6). It is readily noted that horizontal array deflection is most severe for the bow aspect. The stern aspect appears to be less severe, with the beam and mixed wind and seas aspects showing the smallest array departure in the horizontal plane.

Before suggesting probable causes for the above-discussed array perturbations, consider the bow-on case represented in Fig. 10. This figure represents a composite plan view

Table 3. Wind and sea effects.

WIND & SEAS ASPECT	FORCE	CSE STEERED THROUGH THE WATER (DEG)	CSE MADE GOOD OVER GROUND (DEG)	△CSE (DEG)	AVE HORIZONTAL ARRAY DEFLECTION (DEG)	TRACK
BOW	GENTLE	050	018	32	17	L29-L30
BOW	MODERATE	028	020	8	5	B2-L26
BOW	MODERATE	055	043	12	Variable	L27-L28
BOW	STRONG	092	114	22	5 (½)	L8-L9(2)
STERN	GENTLE	247	249	2	3 (½)	L6-L7
STERN	MODERATE	212	198	14	11	B1-B2
STERN	MODERATE	225	231	6	3	L26-L27
BEAM	MODERATE	137	159	22	2	L28-L29
BEAM	MODERATE	138	172	34	3 (½)	L7-L8
MIXED (BB)	LIGHT	099	091	8	2 (½)	A1-A2
MIXED (BB)	LIGHT	265	269	4	0 (½)	A2-L5
MIXED (BS)	LIGHT	304	280	24	2 (½)	L5-L6
MIXED (BB)	STRONG	101	114	13	2 (½)	L8-L9(1)

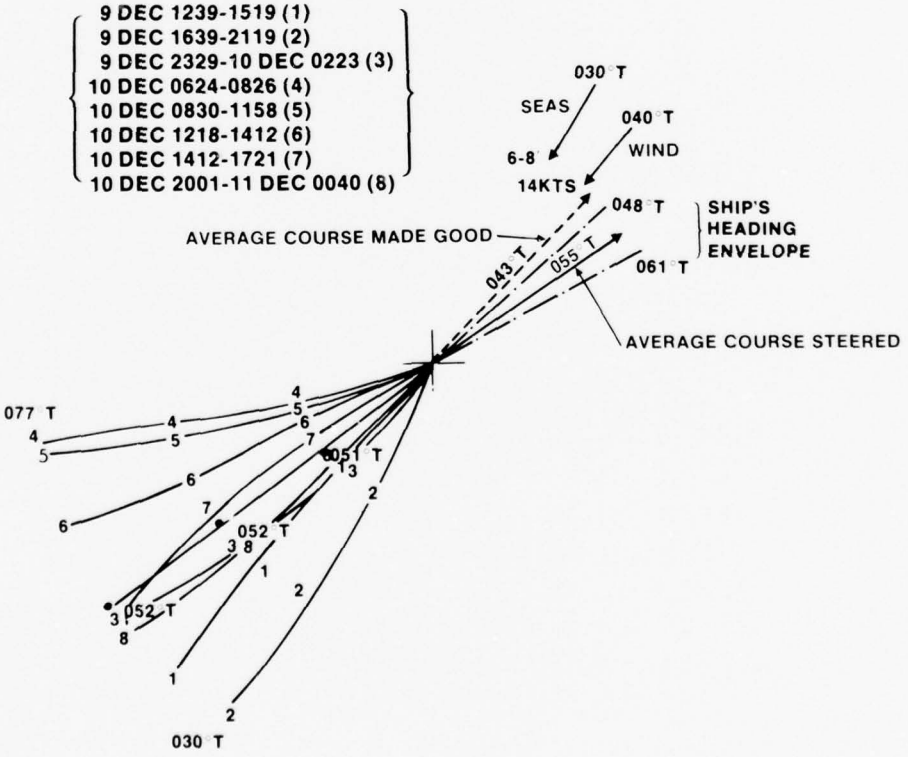

Figure 10. Wind and sea effects L27-L28.

of SEISMIC's averaged headings and resulting averaged array shapes. It is important to note here that although the ship's average heading varied only 13 deg over a 30-hour period, the array was in a nearly constant state of flux in the horizontal plane throughout the period. Vertical migration was noted as well for similar time periods (see Table 4), but degradation of array shape in the vertical plane was not as severe. Further, recall from Table 1 that all eight cases considered for the L27-L28 track passed the linear regression hypothesis. Before leaving this case, it is important to point out the danger of relying solely on data averaging techniques applied blindly over a long period of time. For example, from Fig. 10, it can be seen that the average array-heading deviation for the entire 30-hour period was only 1 deg (051°-052°-052°, respectively for sensors 1, 3 and 5). Hence, excessive averaging can lead to spurious results!

The question still remains, however, why is array deformation more severe for the bow on stern aspects? A logical, albeit not totally documented, answer to this question is that ship pitch is more detrimental to array control than ship roll. This conclusion is intuitively appealing since positive ship speed control is nearly an impossibility for a conventional propeller-driven, shallow-draft, keel-less hull ship heading at slow speed into or with the seas. The key to positive array control then, is to minimize ship speed and, hence, array speed variability. Possible solutions to this perplexing problem will be discussed later.

Table 4. Vertical displacement profiles B1–L30.

TRACK	TIME (ZULU)	AVE DEPTH READINGS (m) 2	3	5	△DPH (m) 5 - 2	TILT ◁ (DEG)	AVE SHIP SPD (KTS)	AVE SPD OVR GND (KTS)	WIRE SCOPE (FT)
B1-B2	0758-1100	326	335	366	40	1.2	1.9	2.3	1650
B2-L26	1545-2025	365	400	431	66	2.0	2.3	2.1	1650
L26-L27	0818-1339	413	438	486	73	2.2	1.9		1800
	1359-0349	426	457	508	82	2.7	1.9	2.6	1800
	0458-0858	334	350	377	43	1.3	1.7		1800
		(408)		(481)		(2.2)	(1.9)		
L27-L28	1239-1619	519	568	658	139	4.3	2.3		
	1639-2119	437	482	546	109	3.3	2.1		
	2329-0223	395	—	459	64	2.0	1.8		
	0624-0858	435	483	556	121	3.7	1.6	1.8	1800
	0858-1158	408	436	490	82	2.6	2.0		
	1218-1412	416	459	544	128	3.9	2.3		
	1412-1801	388	430	488	100	3.1	2.2		
	2001-0040	472	509	578	106	3.3	2.0		
		(439)		(545)		(3.4)	(2.1)		
L28-L29	0220-0500	352	—	410	58	1.7	2.1	2.1	1800
L29-L30	0659-1243	434	—	518	84	2.5	1.8	2.7	1800

TURNING PROFILES AND ARRAY SETTLING TIME

Maintaining constant array speed is extremely critical during change of course evolutions. Here, loss of ship speed inherently results in a further sinking of the array (Table 5). If the loss of ship speed during a turning evolution is severe, i.e., of the order of $\geqslant 0.3$ knots for tow speeds of less than 3 knots, the array will effectively become dead-in-the-water (DIW) and settle at an alarming rate (see Fig. 6). This phenomenon is directly related to depth and becomes critical with deep tows, i.e., tows in excess of 600 m. This condition is due in part to the increased compressibility of the array with increasing depth (Fig. 11).

Table 5. Turning profiles.

△ SPD (KTS)	△ TIME CSE CHG (HRS)	△ TIME ARRAY MAX (HRS)	△ TIME ARRAY VERT (HRS)	△ TIME ARRAY HORIZ (HRS)	INITIAL DEPTH (AVE) (M)	△ DEPTH AVE (M)	△ TILT (DEG)	△ CSE CHG (DEG)	△ ARRAY HEADING (DEG)	STATION
0.8	1.7	2.5	2.5	2.5	714	12	0.5	75	79	L7
0.6	0.8	1.7	1.3	1.7	517	156	2.0	78	130	L28
0.6	0.4	3.1	2.9	2.7	299	302	3.7	184	199	L27
0.4	0.4	3.2	2.2	3.2	751	18	0.8	55	42	L6
0.0	1.1	2.0	2.0	1.8	414	110	0.4	85	125	L29
0.3	—	5.6	3.8	5.6	331	10	0.2	180	173	B2
* 0.4	1.1	1.5	1.4	1.5	232	269	3.6	167	180	A2
0.8	1.0	4.1	4.1	3.8	789	168	2.2	21	65	L8
1.5	0.9	5.1	4.1	5.1	534	298	3.3	34	14	L5

* **Scope change conducted concurrently**

Maintaining constant ship speed during turning evolutions appears to be a practical means of minimizing array settling time during turning evolutions. If the array has little or no effect on the ship during ship turns, then maintaining constant ship speed would be a simple matter. Unfortunately, this condition does not exist, and in reality, an array of the order of size magnitude of LAMBDA tends to act as a large sea anchor, especially during large array heading changes. The result, then, is that any loss of ship speed during turning evolutions is extremely detrimental, i.e., produces array deformation and increases settling time. This result may be observed by examining several of the turning profiles in the time series plots of Appendix A, Table 5, and Fig. 12 and noting that the array generally tends to settle further in the water column with drop in ship speed during turning evolutions.

As a possible solution to this problem, some prudent seamanship tactics were employed. At station L28, as a first guess at maintaining constant array speed, it was decided to increase ship speed by approximately 0.5 knots 15 min prior to commencement of the

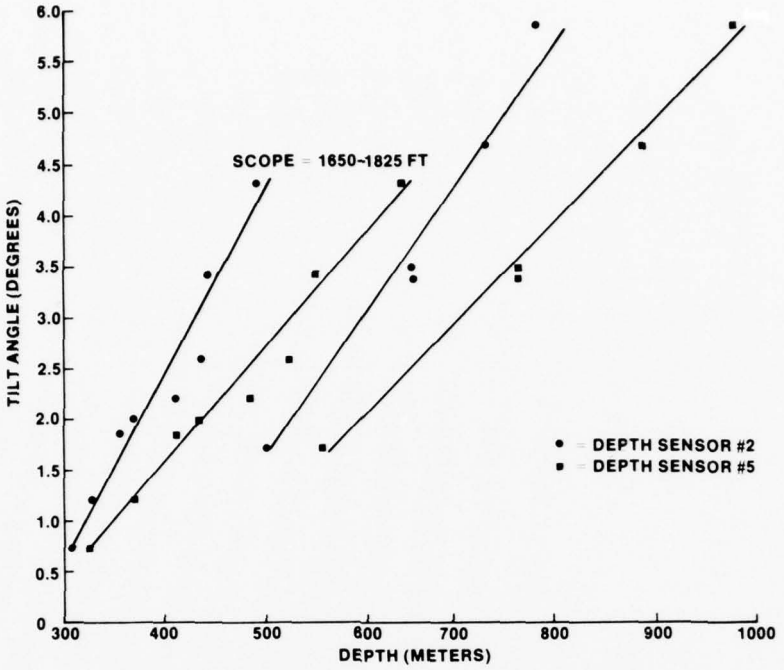

Figure 11. Tilt angle as a function of depth.

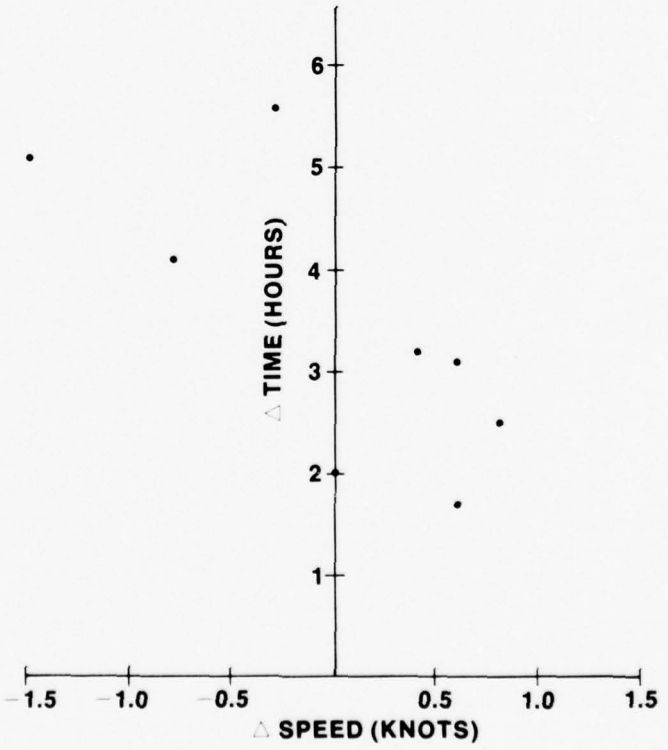

Figure 12. Change in ship speed as a function of array settling time.

turning evolution (Fig. 12). This time interval approximated the time for the speed increase to be felt by the array. Thus, it was hoped that the array would have a net increase in speed and momentum as the ship commenced its turn. Additionally, rather than allow the array to diminish the ship's speed through the turn, as had been the normal practice during the exercise, it was decided to maintain the positive speed differential through the entire duration of the turning evolution. As seen from Fig. 13, the result was more pronounced than anticipated in that the average array depth decreased by approximately 150 m. Of importance though, is the fact that one of the desired effects was achieved; array settling time was greatly reduced (see Table 5). A more gentle approach was adopted at station L29. Here it was decided to try to maintain constant ship speed through the entire turn by adding the requisite number of shaft turns at the first indication of diminished ship speed as sensed by the installed knot meter read directly on the bridge of the ship. A certain amount of nautical guesswork (seaman's eye) was employed in sensing the proper number of shaft revolutions to be added in order to maintain constant ship speed. Figure 14 reflects the desired result: array depth remained relatively constant during the turning evolution, and settling time showed a marked improvement. Unfortunately, this turning evolution, for all intents and purposes, marked the termination of documentable turning evolutions for the exercise, and no further seamanship tactics could be attempted. Nonetheless, it is clear that positive effort devoted to preserving, at a minimum, constant ship speed through turning evolutions results in minimizing array deformation by maintaining nearly constant array depth and reducing array settling time.

CONCLUSIONS

Positive ship speed control is absolutely essential to minimize array deformation. Ideally, ignoring the possibility of underwater currents, misballisted modules, etc., constant ship speed should allow for the perfect case of straight-line towing. At the very minimum, the influences of ship, and array speeds can be minimized by maintaining constant ship speed, which will permit a more thorough and qualitative analysis of the other parameters affecting array dynamics.

During turning evolutions, array deformation is maximum, and positive ship speed control is extremely critical in order to minimize array stabilization time. Any incremental loss of ship/array speed at these critical times results in a definite prolonging of array stabilization time. Conversely, a slight (≤ 0.5 knot) increase in net ship speed may significantly decrease array deformation time. However, further testing of this hypothesis is required before drawing any firm conclusion on the merit of incremental ship-speed increase.

Absolute control of array dynamics is heavily sea-state and ship-aspect dependent. For the conventional "mud" boat configuration considered in this report, the bow-on and trailing-seas aspects produced the most pronounced effect on array deformation due to the inability of the ship to maintain continual positive speed control. Ship pitch is apparently much more detrimental to positive ship speed control than ship roll. Further, once a course made good has been established, the ship's automatic pilot should be engaged and a rigid "hands-off" policy observed, lest a straight course will not be achievable. Array straightness is much more important than attempts to maintain a precise polygon leg.

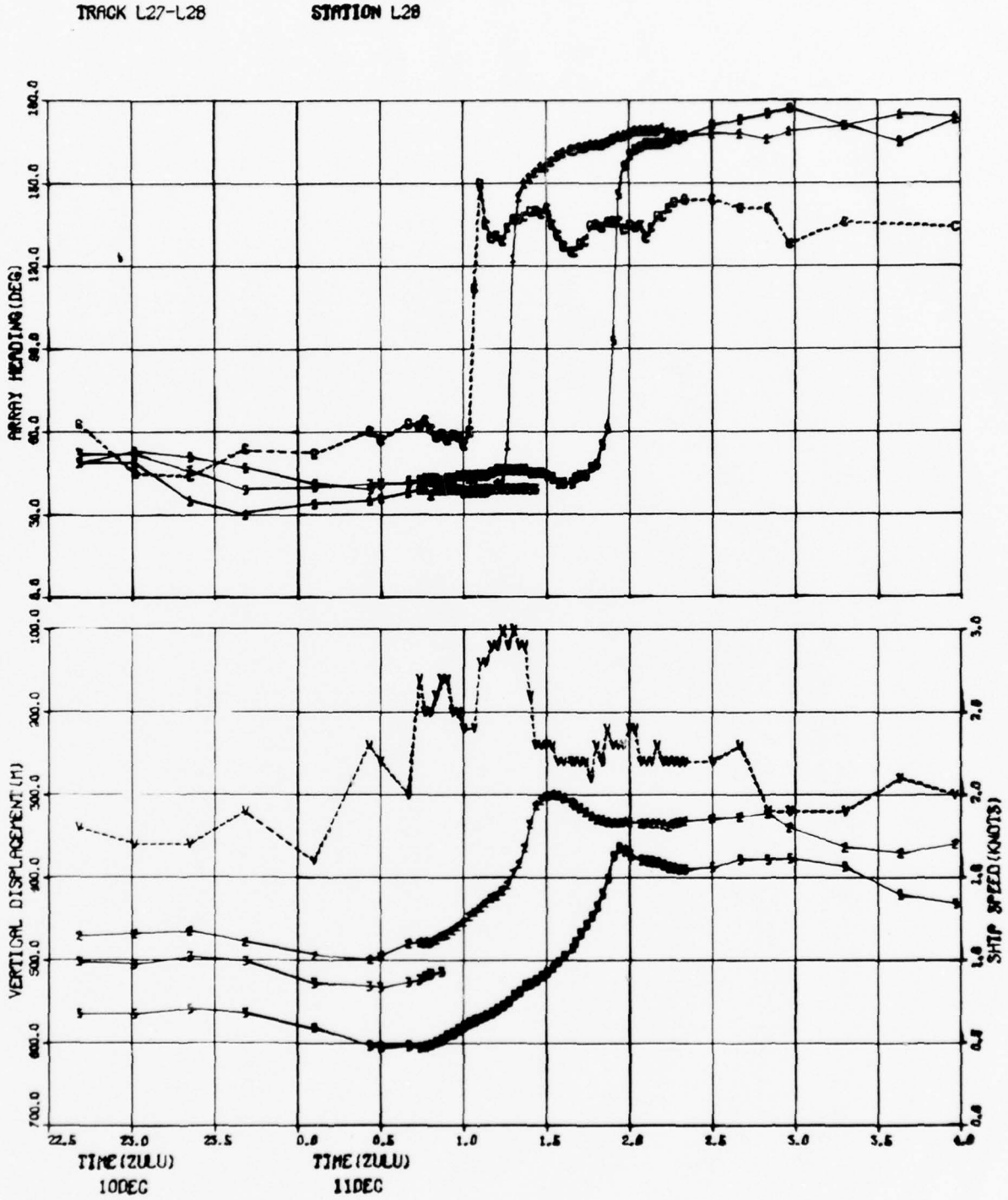

Figure 13. Station L28 turning profile.

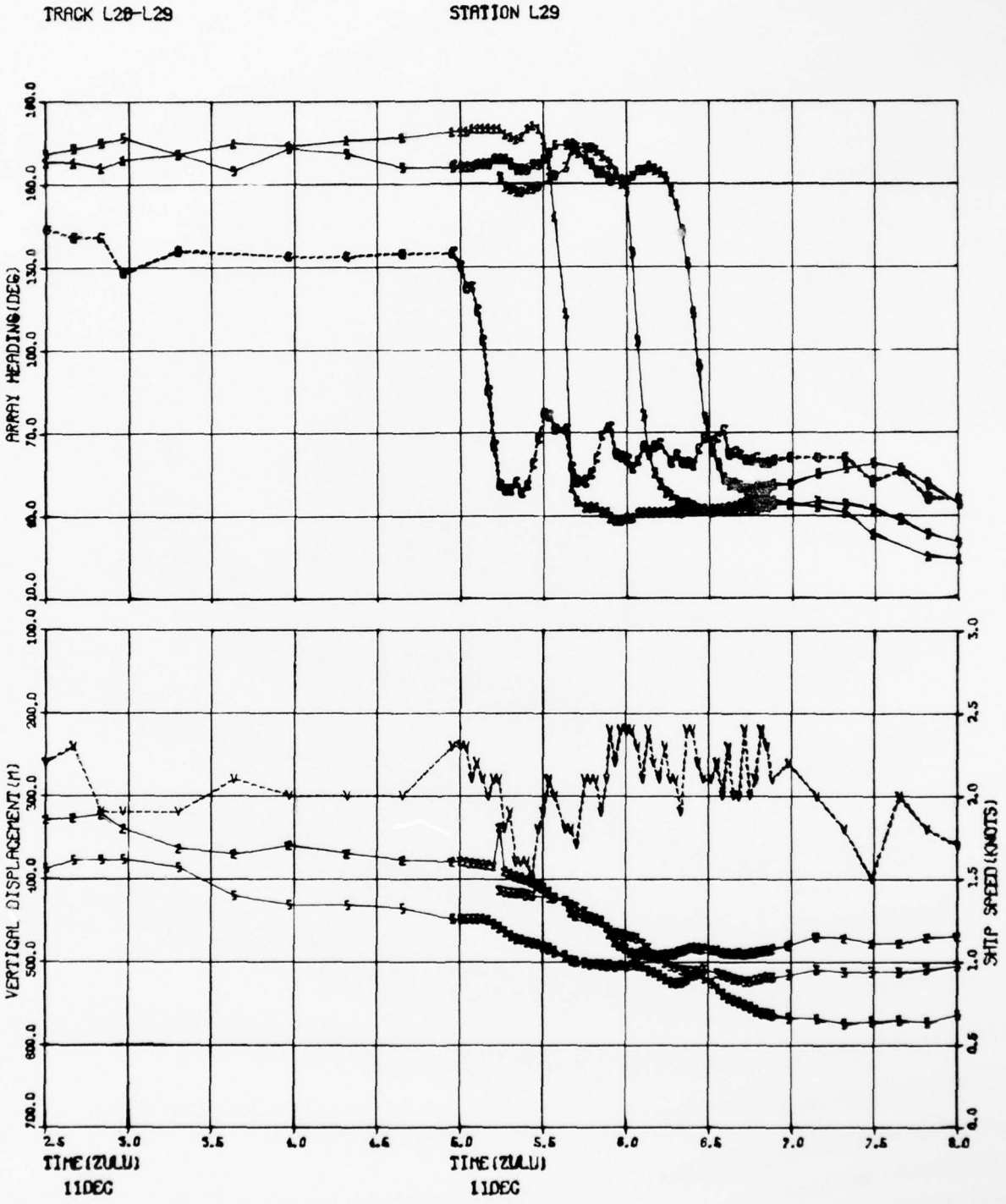

Figure 14. Station L29 turning profile.

Linear regression analysis is a valid candidate in describing vertical array deformation. The corollary argument does not appear to hold merit for the horizontal plane.

Array towing vessels of the SEISMIC EXPLORER type represent an inadequate platform for controlling array dynamics. Deeper draft vessels, having a keel and variable-pitch propeller(s) with large rudder(s), are needed, especially for the employment of long towed arrays in significant sea states, i.e., sea states greater than Beaufort 2. The author recognizes that some trade-off in possible increased noise caused by variable-pitch propellers may have to be accepted.

FUTURE CONSIDERATIONS AND RECOMMENDED AREAS FOR IMPROVEMENT

A detailed study of the effects of ship hull configuration and propulsion type on array dynamics is recommended prior to the large-scale production of long towed arrays. In other words, increased emphasis in defining the "ideal" towing platform is essential, lest the problem of array dynamics remain vague.

Until a better understanding of the parameters that truly affect array dynamics is ascertained, increased monitoring is required. The addition of array tension and vertical wire towing angle sensors would be of tremendous value in measuring changes in ship and array speed. Further, a suite of remote sensors should be installed at the ship control station (bridge). This would allow the ship driver to calibrate his "seaman's eye" through learning which parameters control array stability and therefore permit him to take timely *preventative* action to maintain array stability (i.e., to exercise *prudent* seamanship in a *timely* manner). A suggested suite of sensors on the bridge would include, but not necessarily be limited to, array tension, array depth (fore and aft only), array heading, vertical wire towing angle and/or array speed. Not necessarily required on the bridge, but of significant potential value, would be the addition of a ship roll and ship pitch indicator. Naturally, all of these sensors should be integrated into the existing NADS system for permanent data retention and post analysis.

Of vital importance to the ship's scientific crew is the addition of a computer software package to analyze and plot array dynamics in real time. With this tool, the Chief Scientist could readily and accurately determine the position of the array in the water column at any point in time. Array misballasting, turning evolution tactics, etc., could thus be studied on board and the requisite corrections/adjustments implemented to enhance array dynamics.

With time at sea being at a premium, the need for a computerized array dynamics simulator is clear. In this way, the effects of misballasting (be it random or systematic), seamanship tactics, the effects of sea state, etc., could be studied without the expense of going to sea. The products of such an effort could then be further tested and evaluated during follow-on at-sea operations. In developing such a model, care should be taken to ensure that the simulator is not too unwieldly from both a time and expense point of view.

REFERENCES

1. M. Carlson and R. R. Smith, "Solution of the Steady-State Shape of a Towed Array System Towed at Constant Speed," Naval Undersea Center, Code 302, Intra-Division Memo 601-267 of Jan 1973.

2. R. R. Smith, "Effect of Towed Array Buoyancy on Array Towing Characteristics," Naval Undersea Center, Code 302, Intra-Division Memo 302-277, of Jan 1977.

3. J. L. Johnson and D. Barack, "Investigation of LAMBDA Array Tow Profile for Low Tow Speeds," Naval Undersea Center, Code 822, Intra-Division Memo 822-278, of Apr 1977.

4. James C. Lockwood, *Array Deformation Study*, Computer Sciences Corporation, San Diego, CA, Nov 1977.

5. W. L. Dalton and D. K. Shimoda, *Geometrical Shape of Long Towed Array with Mis-Ballasted Modules*, MAR, Incorporated, Rockville, MD, Mar 1975.

6. N. R. Draper and H. Smith, *Applied Regression Analysis*, John Wiley & Sons, Incorporated, NY, 1966.

7. I. N. Gibra, *Probability and Statistical Inference for Scientists and Engineers*, Prentice-Hall, Incorporated, Englewood Cliffs, NJ, 1973.

8. M. R. Spiegel, *Schaum's Outline of Theory and Problems of Statistics*, McGraw-Hill, Incorporated, NY, 1961.

APPENDIX

TIME SERIES PLOTS

TRACK A1 -A2

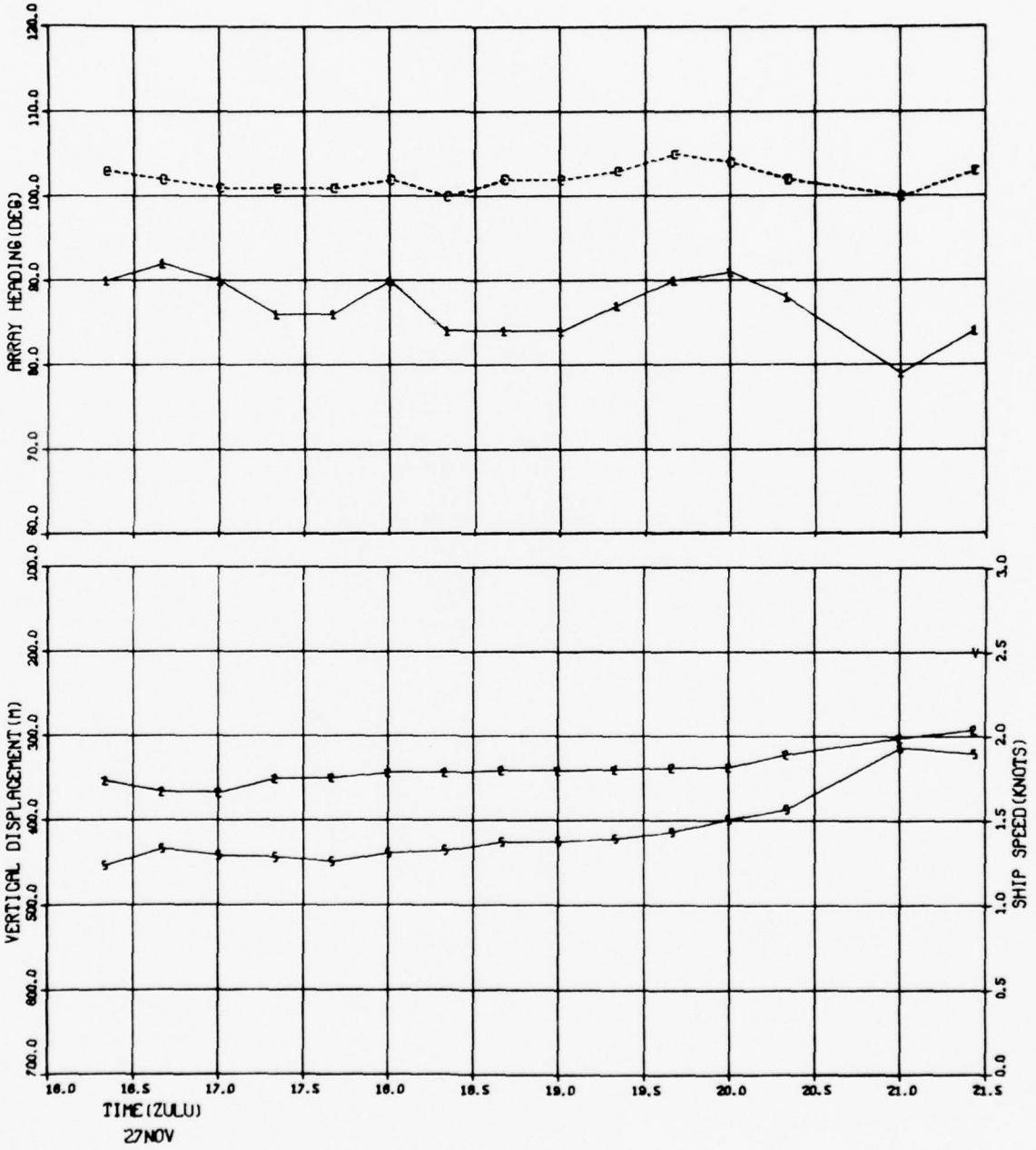
ARRAY HEADING(DEG)
120.0
110.0
100.0
90.0
80.0
70.0
60.0
VERTICAL DISPLACEMENT(M)
100.0
200.0
300.0
400.0
500.0
600.0
700.0
SHIP SPEED(KNOTS)
3.0
2.5
2.0
1.5
1.0
0.5
0.0
16.0
16.5
17.0
17.5
18.0
18.5
19.0
19.5
20.0
20.5
21.0
21.5
TIME(ZULU)
27NOV

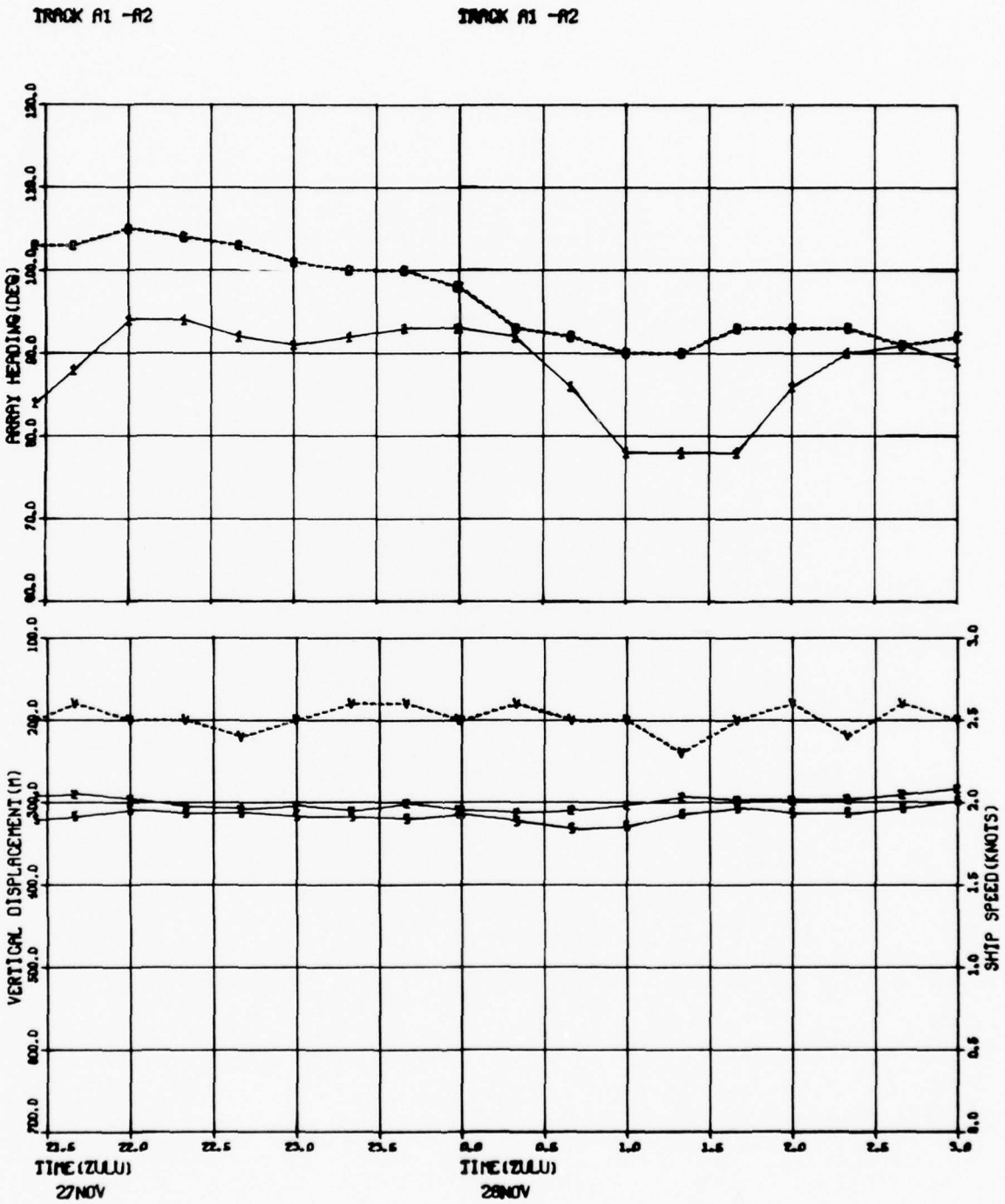
TRACK A1 -A2
TRACK A1 -A2
ARRAY HEADING(DEG)
VERTICAL DISPLACEMENT(M)
SHIP SPEED(KNOTS)
TIME(ZULU)
27NOV
TIME(ZULU)
28NOV

TRACK A1 -A2

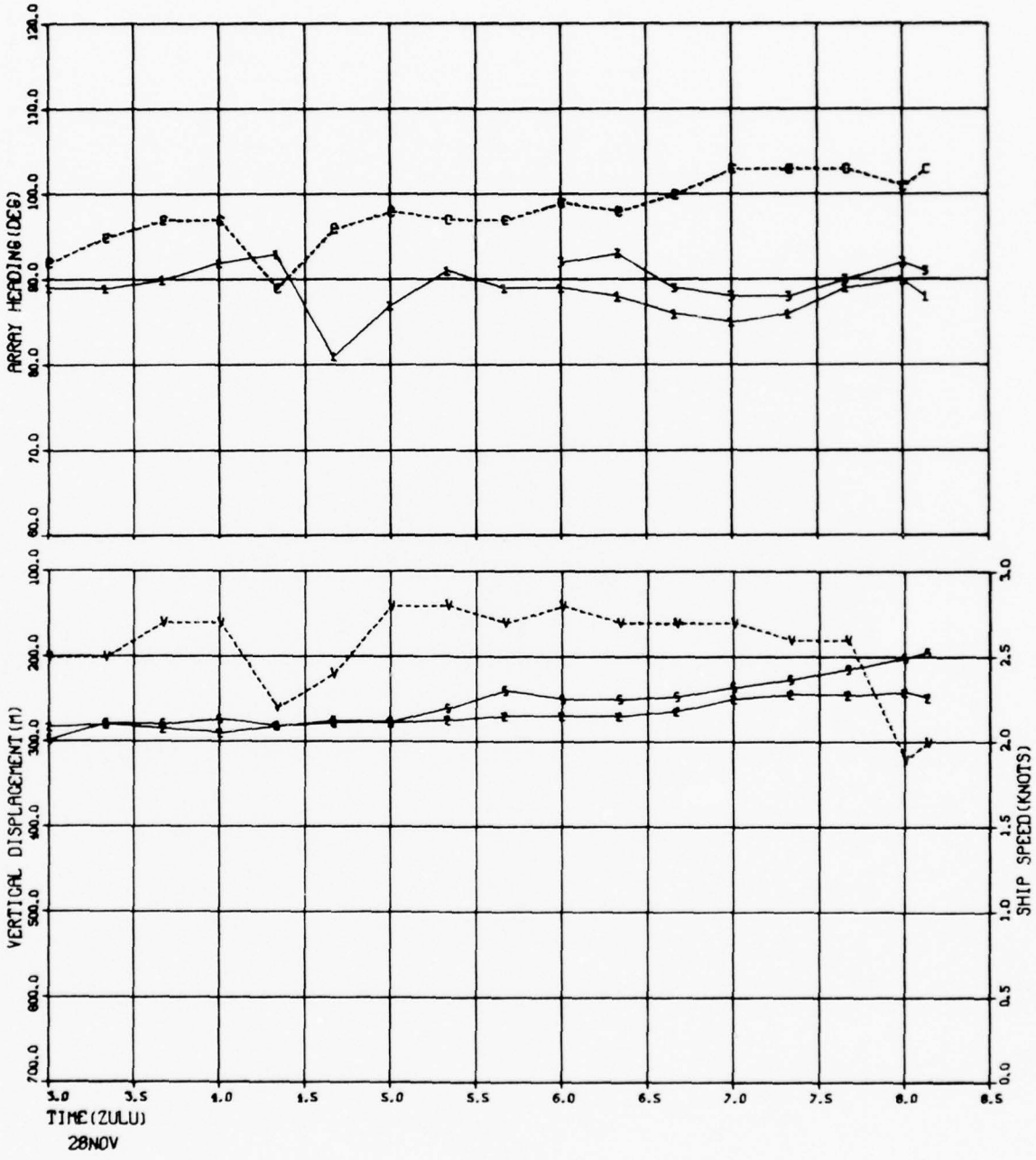
ARRAY HEADING(DEG)
120.0
110.0
100.0
90.0
80.0
70.0
60.0
VERTICAL DISPLACEMENT(M)
100.0
200.0
300.0
400.0
500.0
600.0
700.0
SHIP SPEED(KNOTS)
3.0
2.5
2.0
1.5
1.0
0.5
0.0
3.0
3.5
4.0
4.5
5.0
5.5
6.0
6.5
7.0
7.5
8.0
8.5
TIME(ZULU)
28NOV

STATION A2

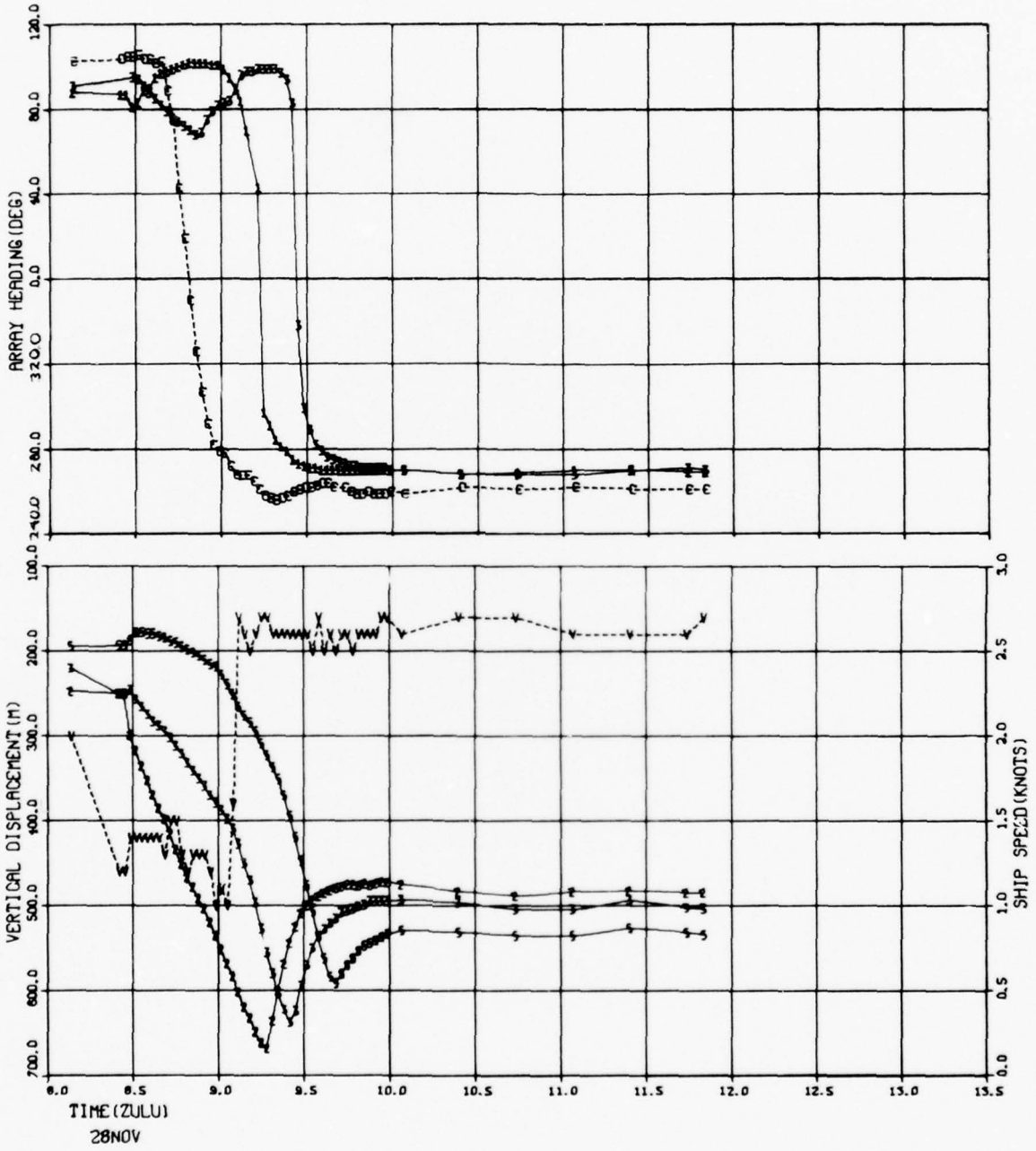
ARRAY HEADING(DEG)
120.0
80.0
40.0
0.0
320.0
280.0
240.0
VERTICAL DISPLACEMENT(M)
100.0
200.0
300.0
400.0
500.0
600.0
700.0
SHIP SPEED(KNOTS)
3.0
2.5
2.0
1.5
1.0
0.5
0.0
8.0
8.5
9.0
9.5
10.0
10.5
11.0
11.5
12.0
12.5
13.0
13.5
TIME(ZULU)
28NOV

STATION LS

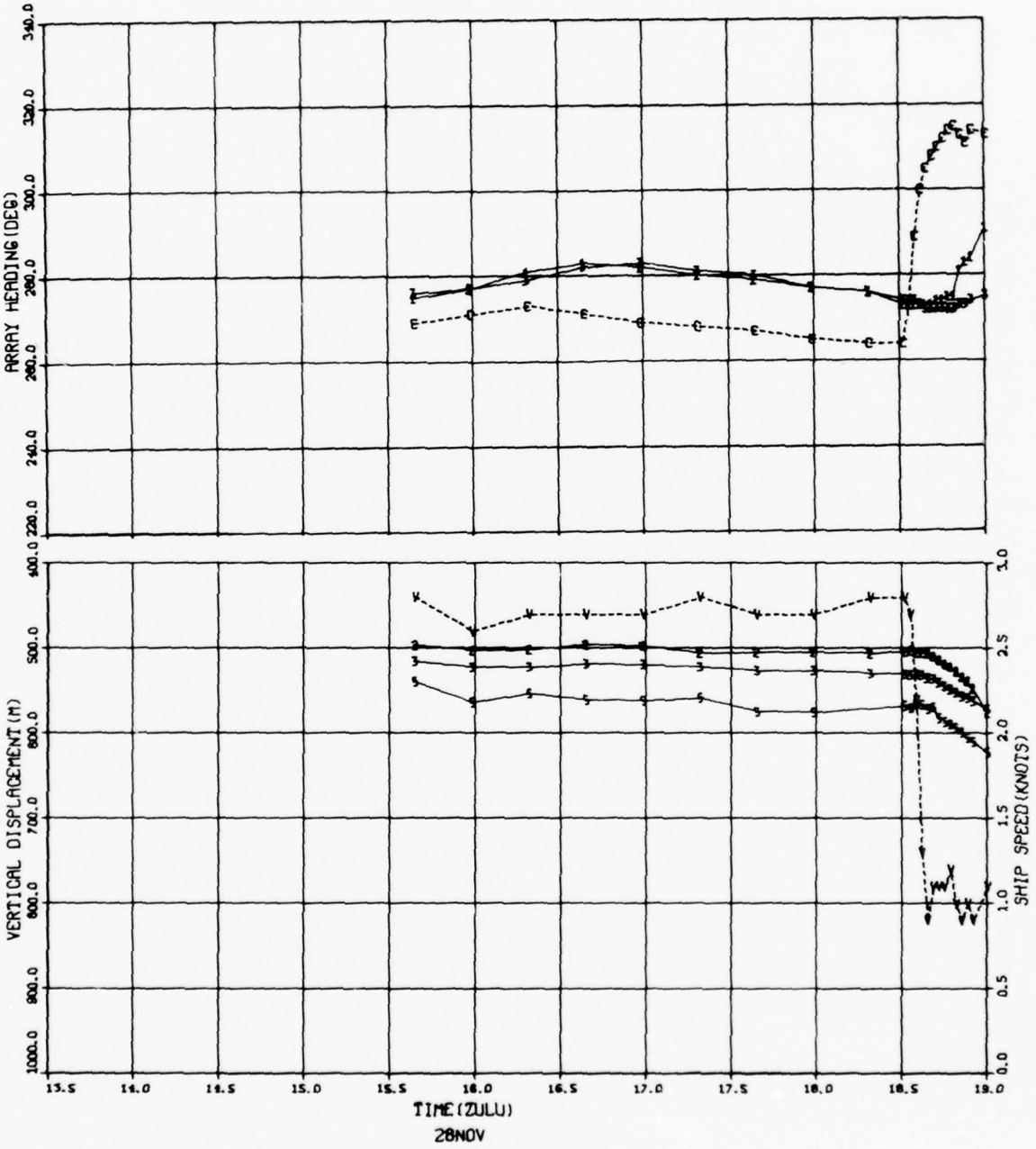
ARRAY HEADING(DEG)
340.0
320.0
300.0
280.0
260.0
240.0
220.0
VERTICAL DISPLACEMENT(M)
400.0
500.0
600.0
700.0
800.0
900.0
1000.0
SHIP SPEED(KNOTS)
3.0
2.5
2.0
1.5
1.0
0.5
0.0
13.5
14.0
14.5
15.0
15.5
16.0
16.5
17.0
17.5
18.0
18.5
19.0
TIME(ZULU)
28NOV

STATION LS

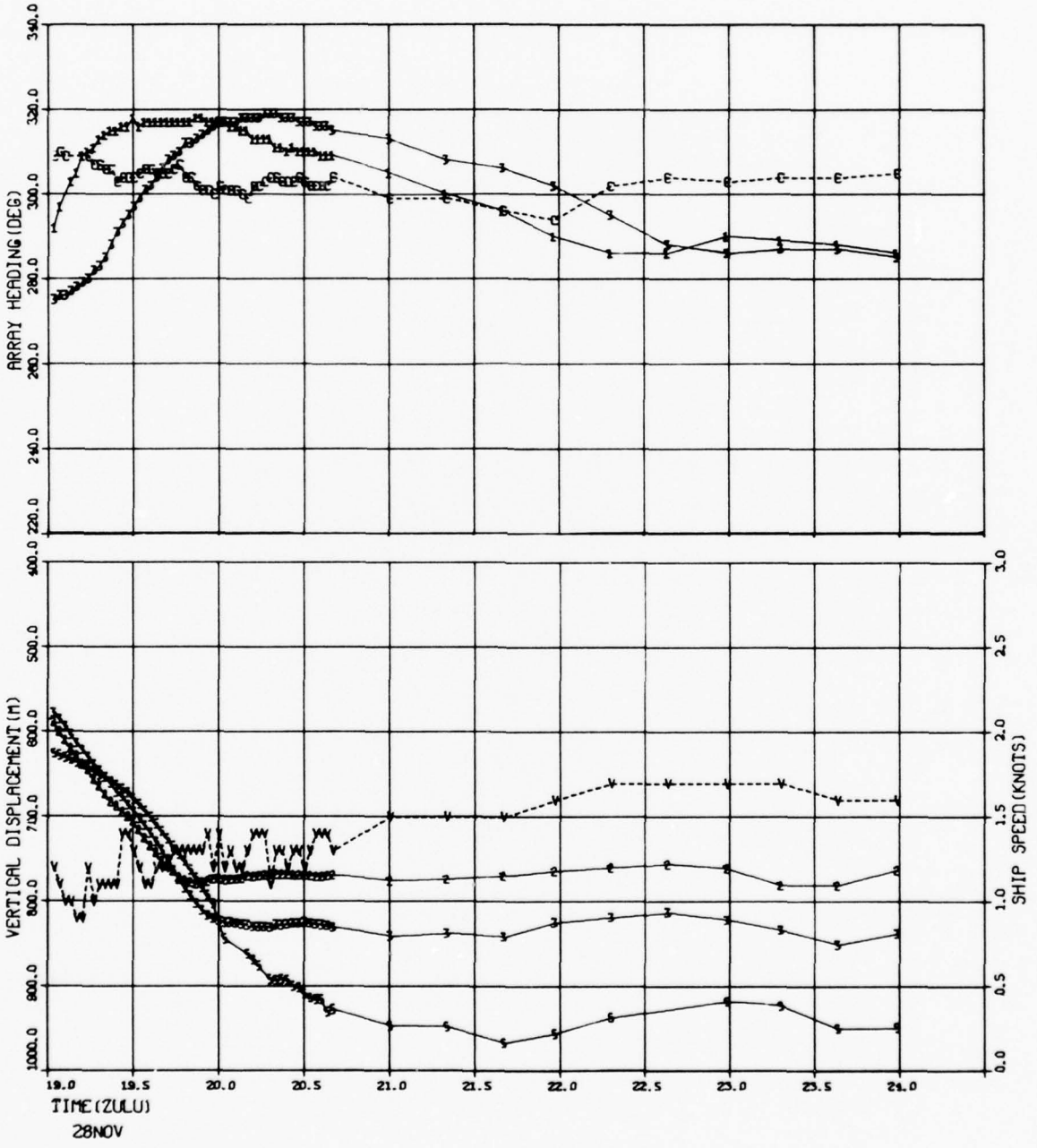
ARRAY HEADING(DEG)
340.0
320.0
300.0
280.0
260.0
240.0
220.0
VERTICAL DISPLACEMENT(M)
400.0
500.0
600.0
700.0
800.0
900.0
1000.0
SHIP SPEED(KNOTS)
3.0
2.5
2.0
1.5
1.0
0.5
0.0
19.0
19.5
20.0
20.5
21.0
21.5
22.0
22.5
23.0
23.5
24.0
TIME(ZULU)
28NOV

TRACK L5 -L6

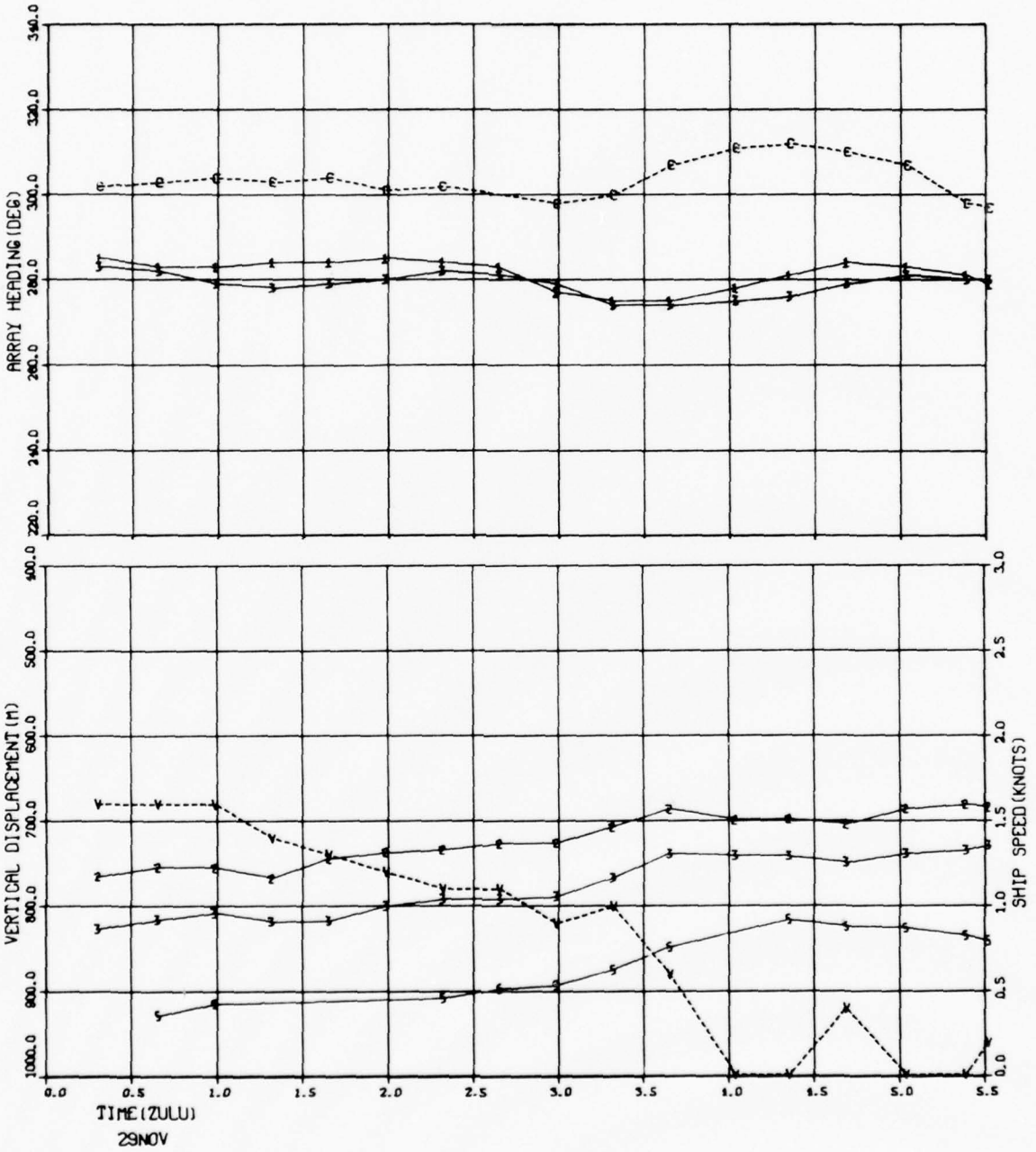
ARRAY HEADING(DEG)
340.0
320.0
300.0
280.0
260.0
240.0
220.0
VERTICAL DISPLACEMENT(M)
400.0
500.0
600.0
700.0
800.0
900.0
1000.0
SHIP SPEED(KNOTS)
3.0
2.5
2.0
1.5
1.0
0.5
0.0
0.0
0.5
1.0
1.5
2.0
2.5
3.0
3.5
4.0
4.5
5.0
5.5
TIME(ZULU)
29NOV

STATION L6

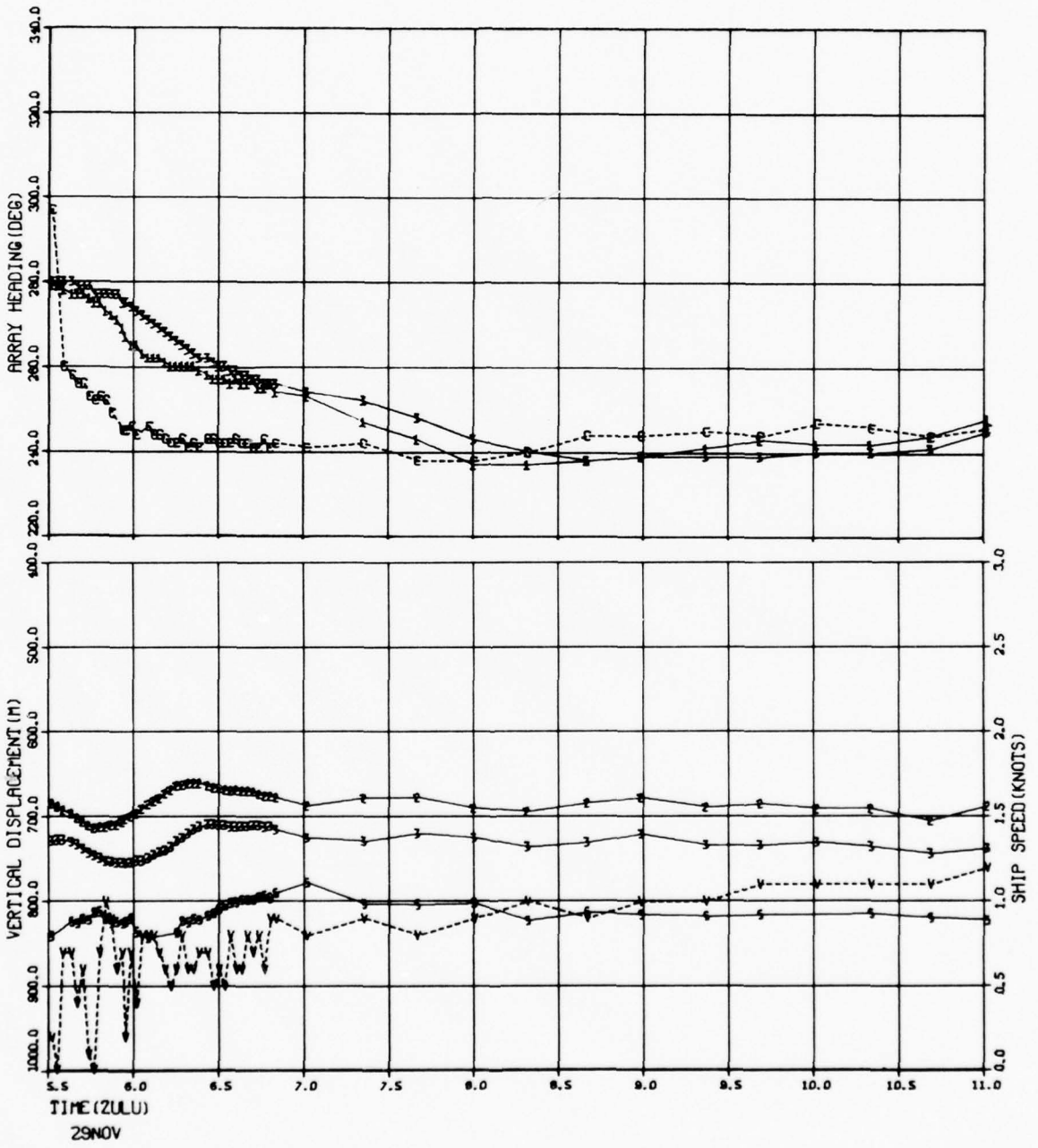
ARRAY HEADING(DEG)
340.0
320.0
300.0
280.0
260.0
240.0
220.0
VERTICAL DISPLACEMENT(M)
400.0
500.0
600.0
700.0
800.0
900.0
1000.0
SHIP SPEED(KNOTS)
3.0
2.5
2.0
1.5
1.0
0.5
0.0
5.5
6.0
6.5
7.0
7.5
8.0
8.5
9.0
9.5
10.0
10.5
11.0
TIME(ZULU)
29NOV

TRACK L6 -L7

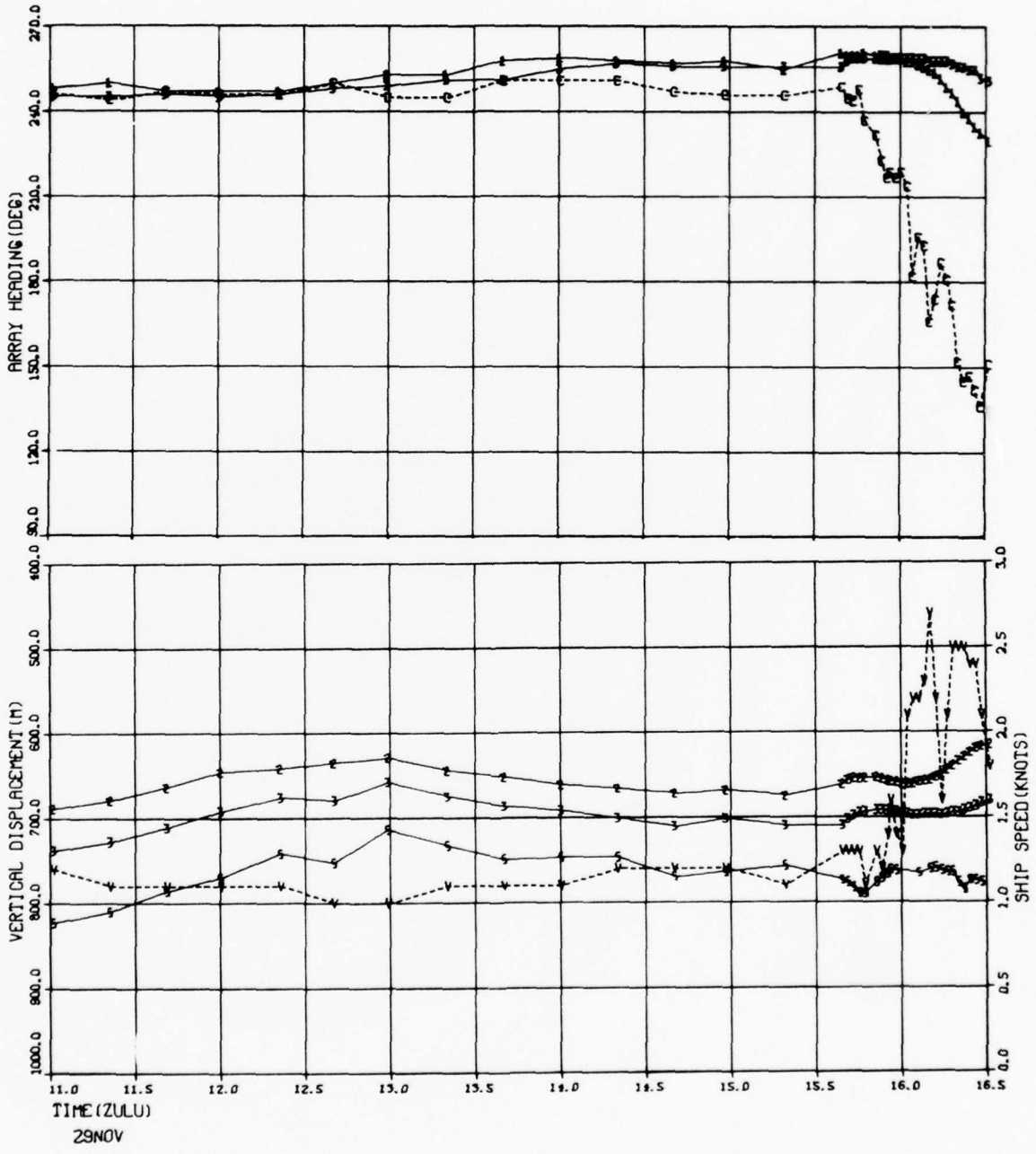
ARRAY HEADING(DEG)
270.0
240.0
210.0
180.0
150.0
120.0
90.0
VERTICAL DISPLACEMENT(M)
400.0
500.0
600.0
700.0
800.0
900.0
1000.0
SHIP SPEED(KNOTS)
3.0
2.5
2.0
1.5
1.0
0.5
0.0
11.0
11.5
12.0
12.5
13.0
13.5
14.0
14.5
15.0
15.5
16.0
16.5
TIME(ZULU)
29NOV

STATION L7

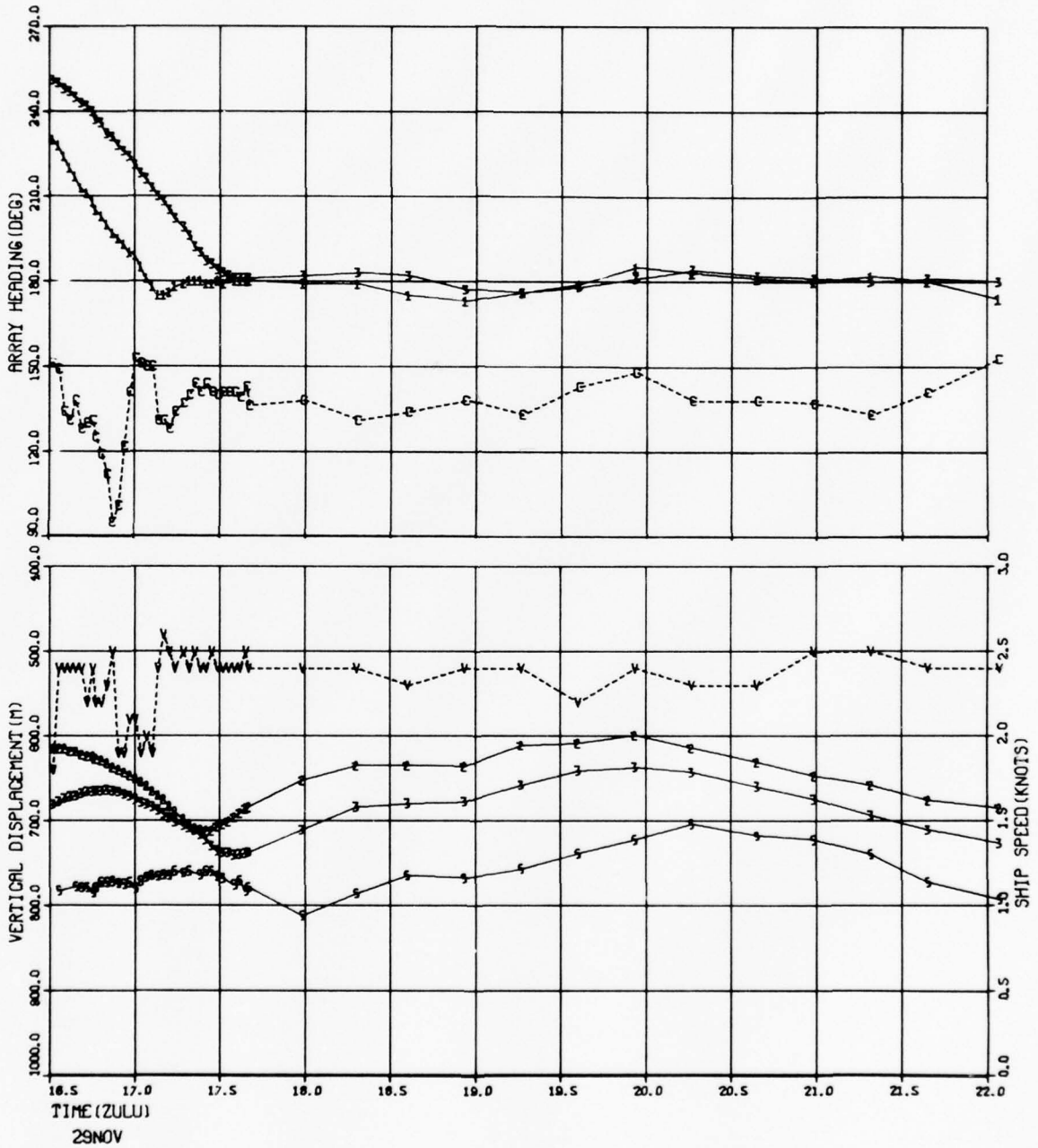
ARRAY HEADING(DEG)
270.0
240.0
210.0
180.0
150.0
120.0
90.0
VERTICAL DISPLACEMENT(M)
400.0
500.0
600.0
700.0
800.0
900.0
1000.0
SHIP SPEED(KNOTS)
3.0
2.5
2.0
1.5
1.0
0.5
0.0
16.5
17.0
17.5
18.0
18.5
19.0
19.5
20.0
20.5
21.0
21.5
22.0
TIME(ZULU)
29NOV

TRACK L7 -L8 STATION L8

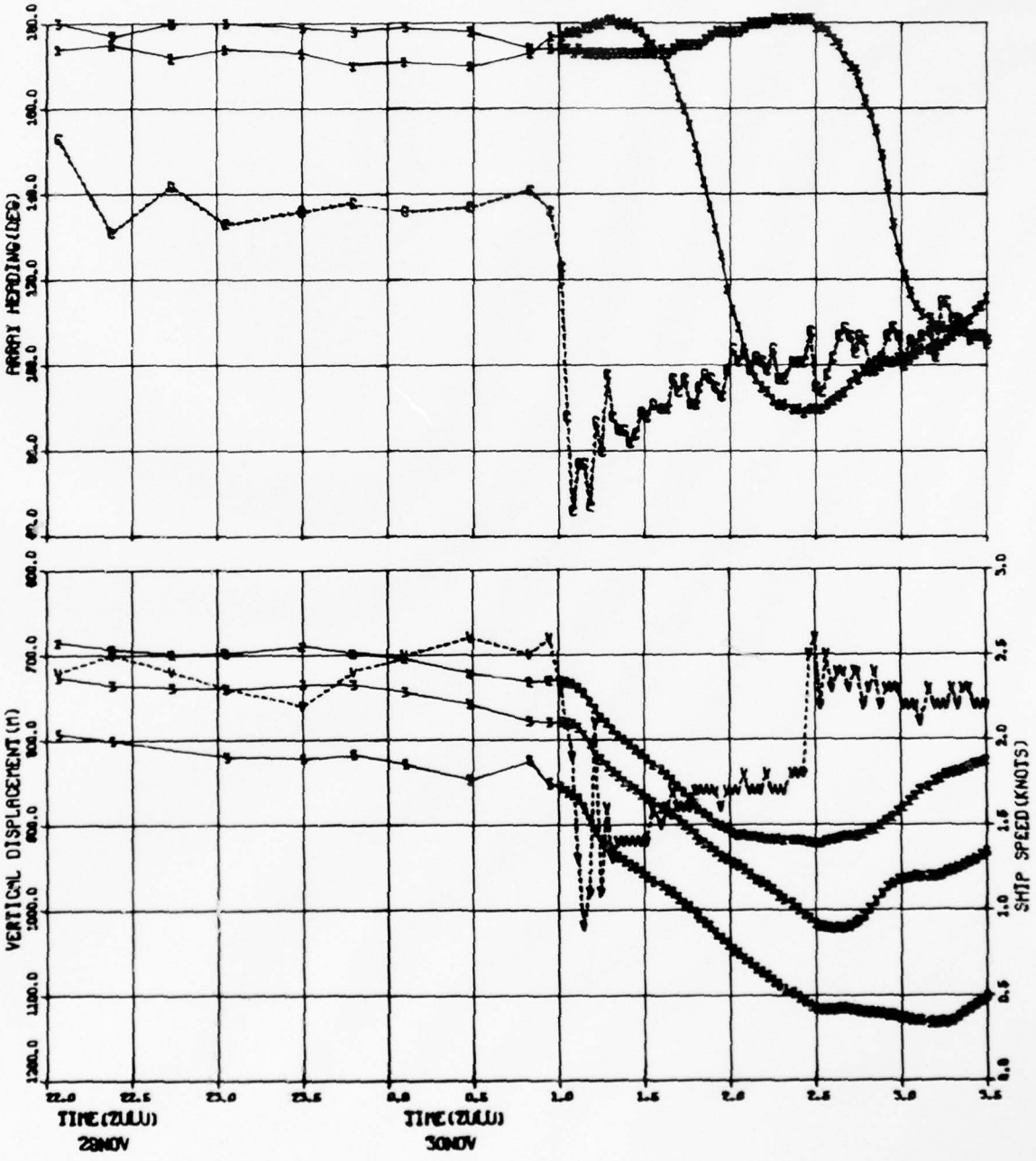

TRACK L8 -L9

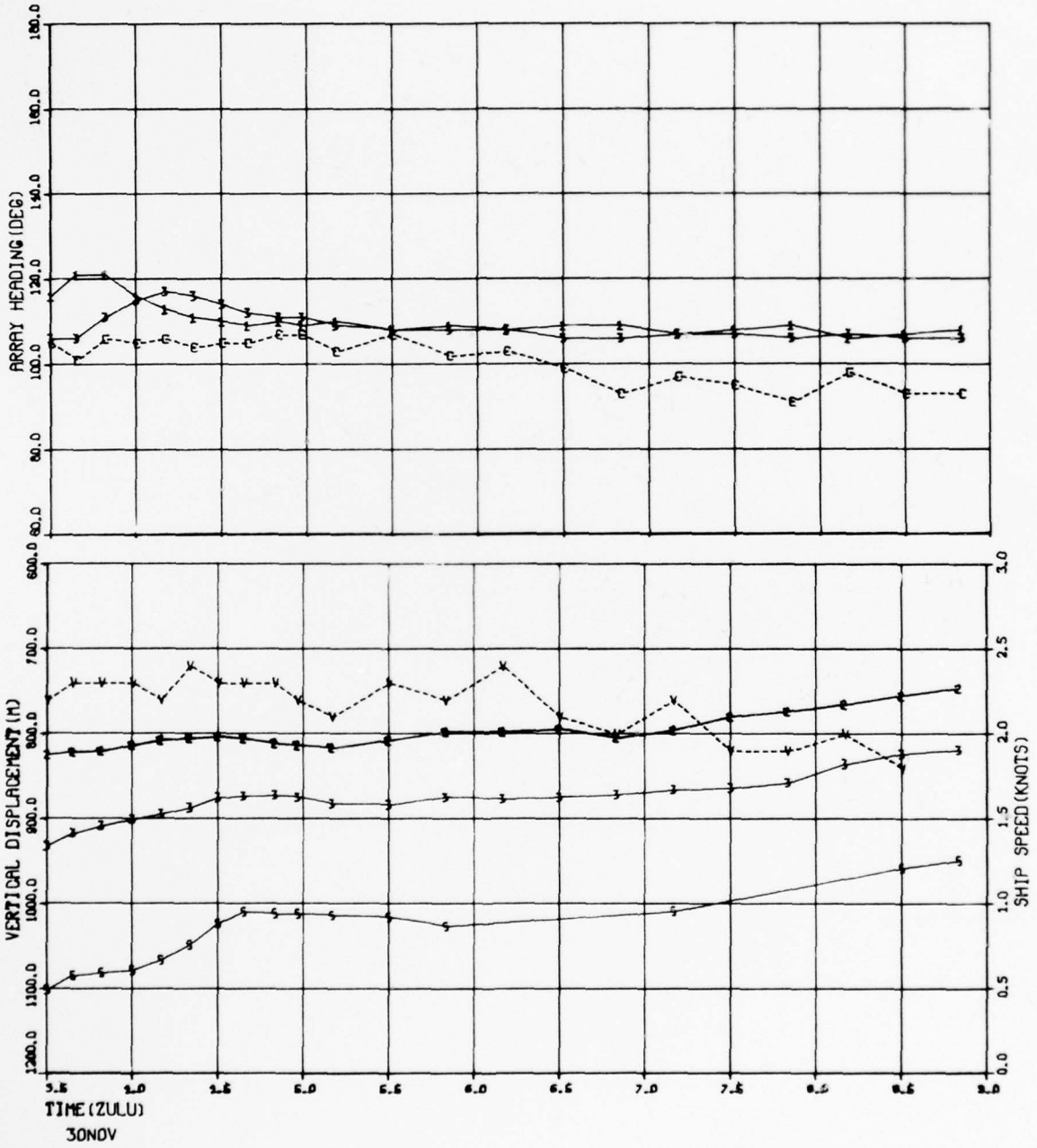
ARRAY HEADING(DEG)
180.0
160.0
140.0
120.0
100.0
80.0
60.0
VERTICAL DISPLACEMENT(M)
600.0
700.0
800.0
900.0
1000.0
1100.0
1200.0
SHIP SPEED(KNOTS)
3.0
2.5
2.0
1.5
1.0
0.5
0.0
5.5
1.0
1.5
6.0
5.5
6.0
6.5
7.0
7.5
8.0
8.5
9.0
TIME(ZULU)
30NOV

TRACK L8 -L9

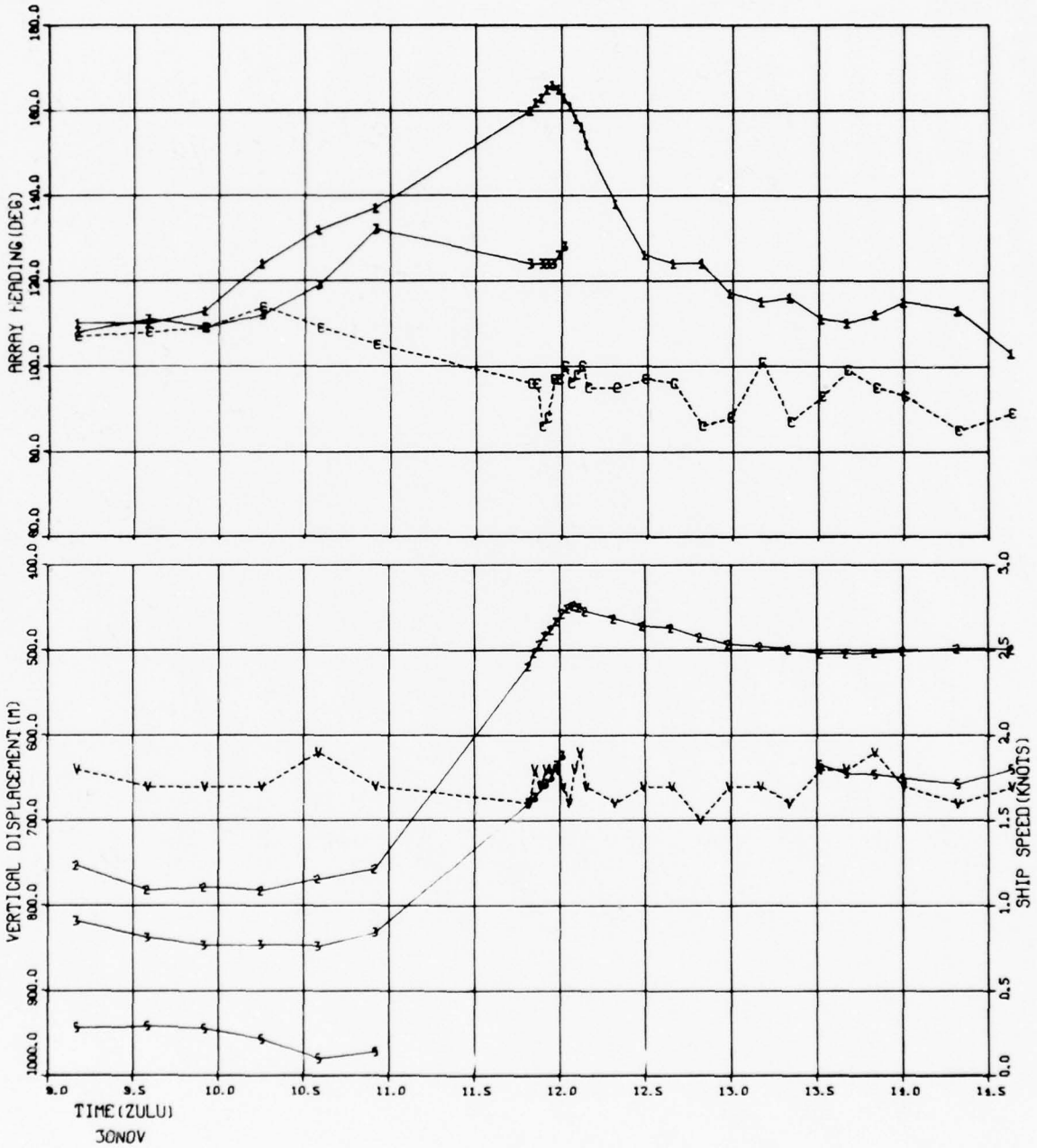
ARRAY HEADING(DEG)
VERTICAL DISPLACEMENT(M)
SHIP SPEED(KNOTS)
TIME(ZULU)
30NOV

TRACK L8 -L9

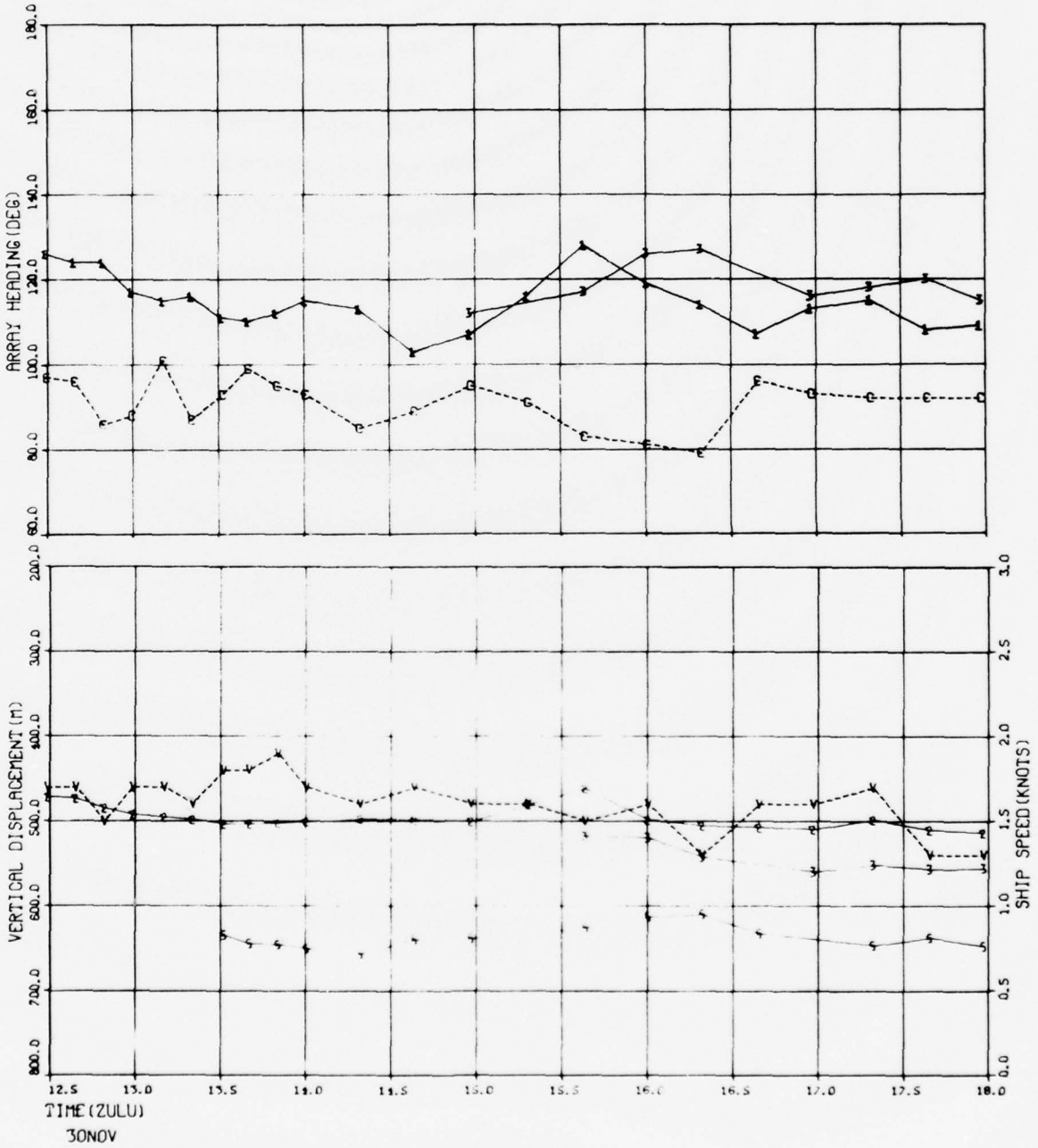
ARRAY HEADING(DEG)
180.0
160.0
140.0
120.0
100.0
80.0
60.0
VERTICAL DISPLACEMENT(M)
200.0
300.0
400.0
500.0
600.0
700.0
800.0
SHIP SPEED(KNOTS)
3.0
2.5
2.0
1.5
1.0
0.5
0.0
12.5
13.0
13.5
14.0
14.5
15.0
15.5
16.0
16.5
17.0
17.5
18.0
TIME(ZULU)
30NOV

TRACK L8 -L9

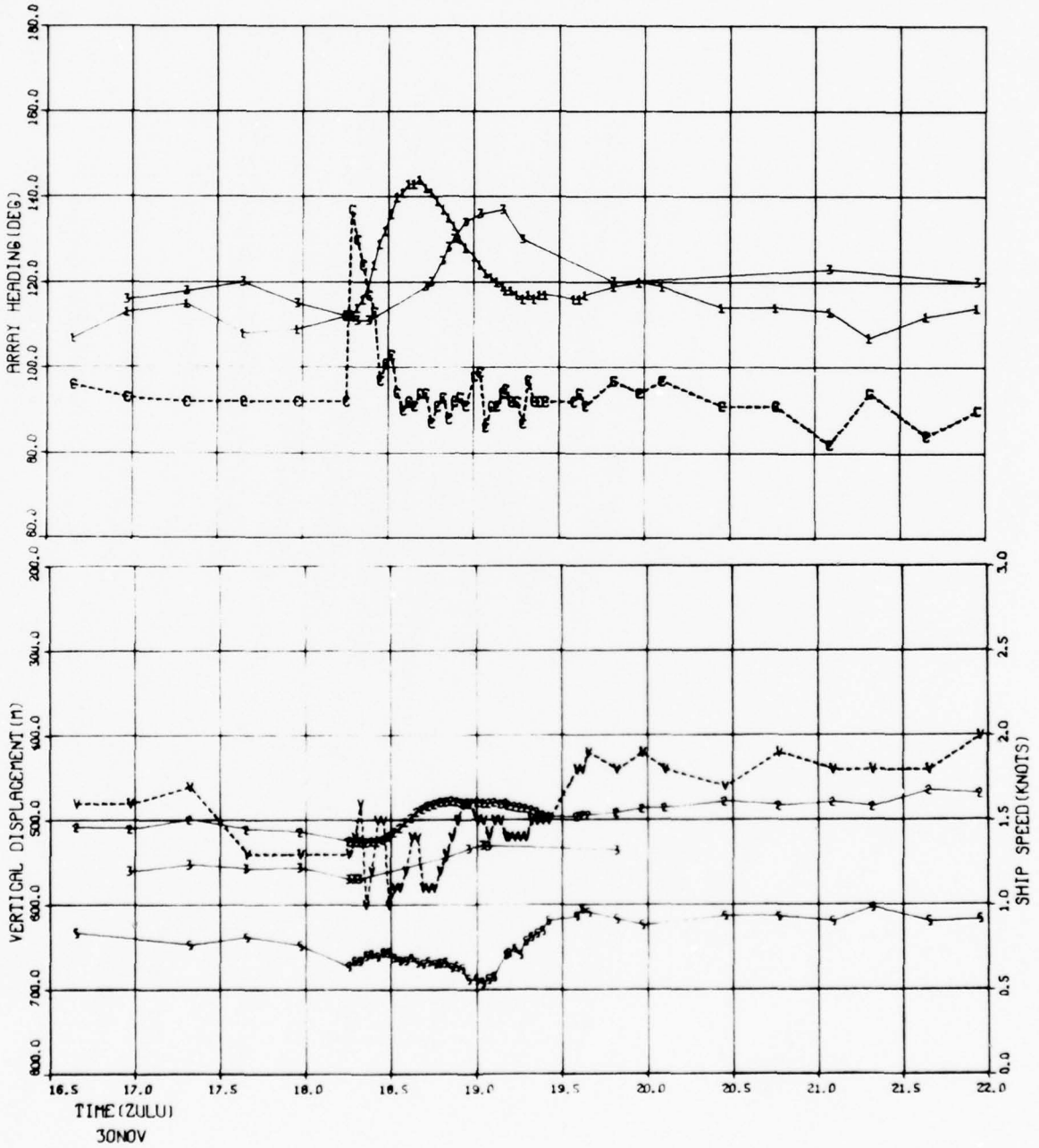
ARRAY HEADING(DEG)
180.0
160.0
140.0
120.0
100.0
80.0
60.0
VERTICAL DISPLACEMENT(M)
200.0
300.0
400.0
500.0
600.0
700.0
800.0
SHIP SPEED(KNOTS)
3.0
2.5
2.0
1.5
1.0
0.5
0.0
16.5
17.0
17.5
18.0
18.5
19.0
19.5
20.0
20.5
21.0
21.5
22.0
TIME(ZULU)
30NOV

TRACK B1 -B2

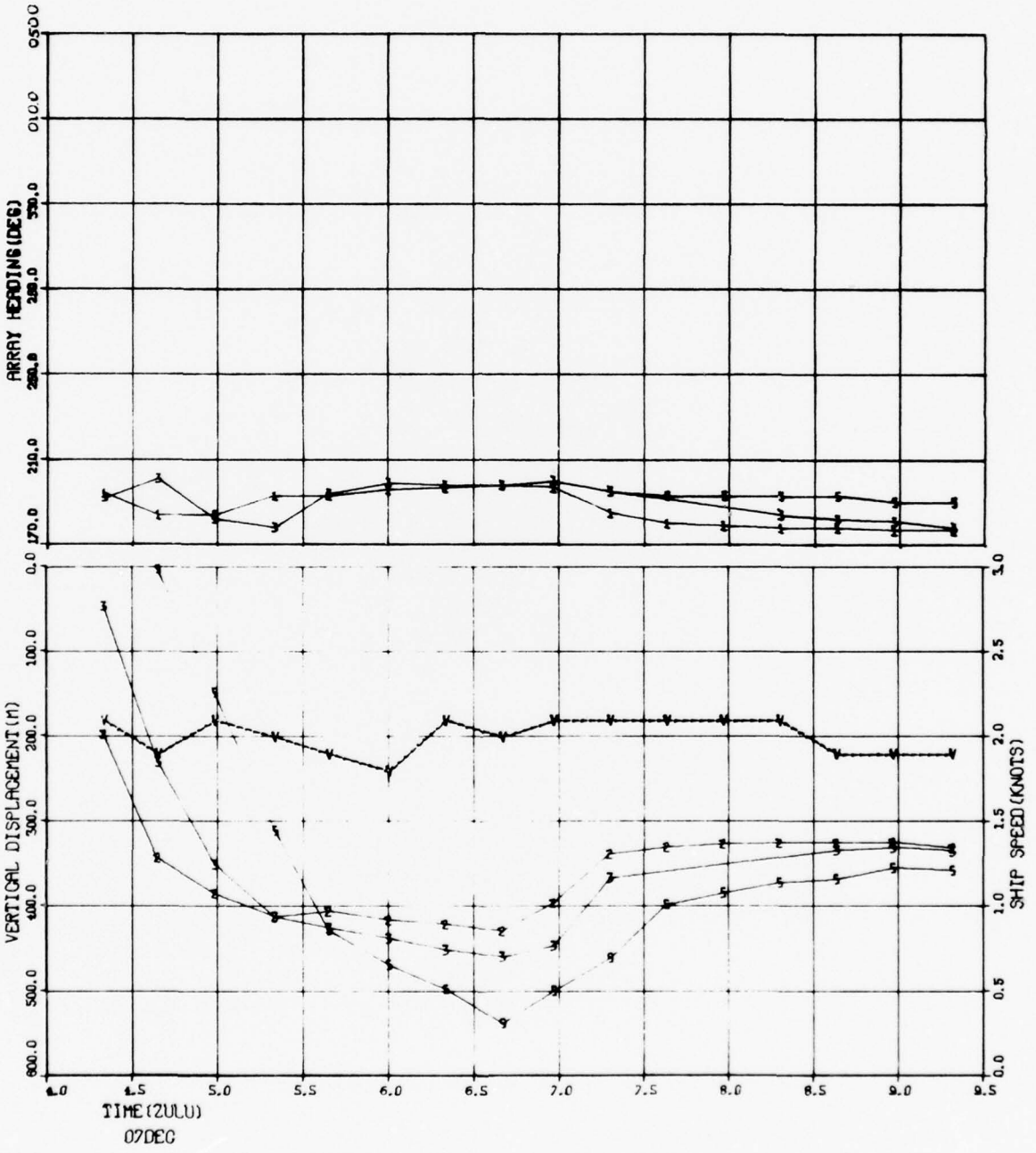
ARRAY HEADING(DEG)
0500
0100
350.0
280.0
210.0
170.0
VERTICAL DISPLACEMENT(M)
0.0
100.0
200.0
300.0
400.0
500.0
800.0
SHIP SPEED(KNOTS)
3.0
2.5
2.0
1.5
1.0
0.5
0.0
4.0
4.5
5.0
5.5
6.0
6.5
7.0
7.5
8.0
8.5
9.0
9.5
TIME(ZULU)
07DEC

STATION B2

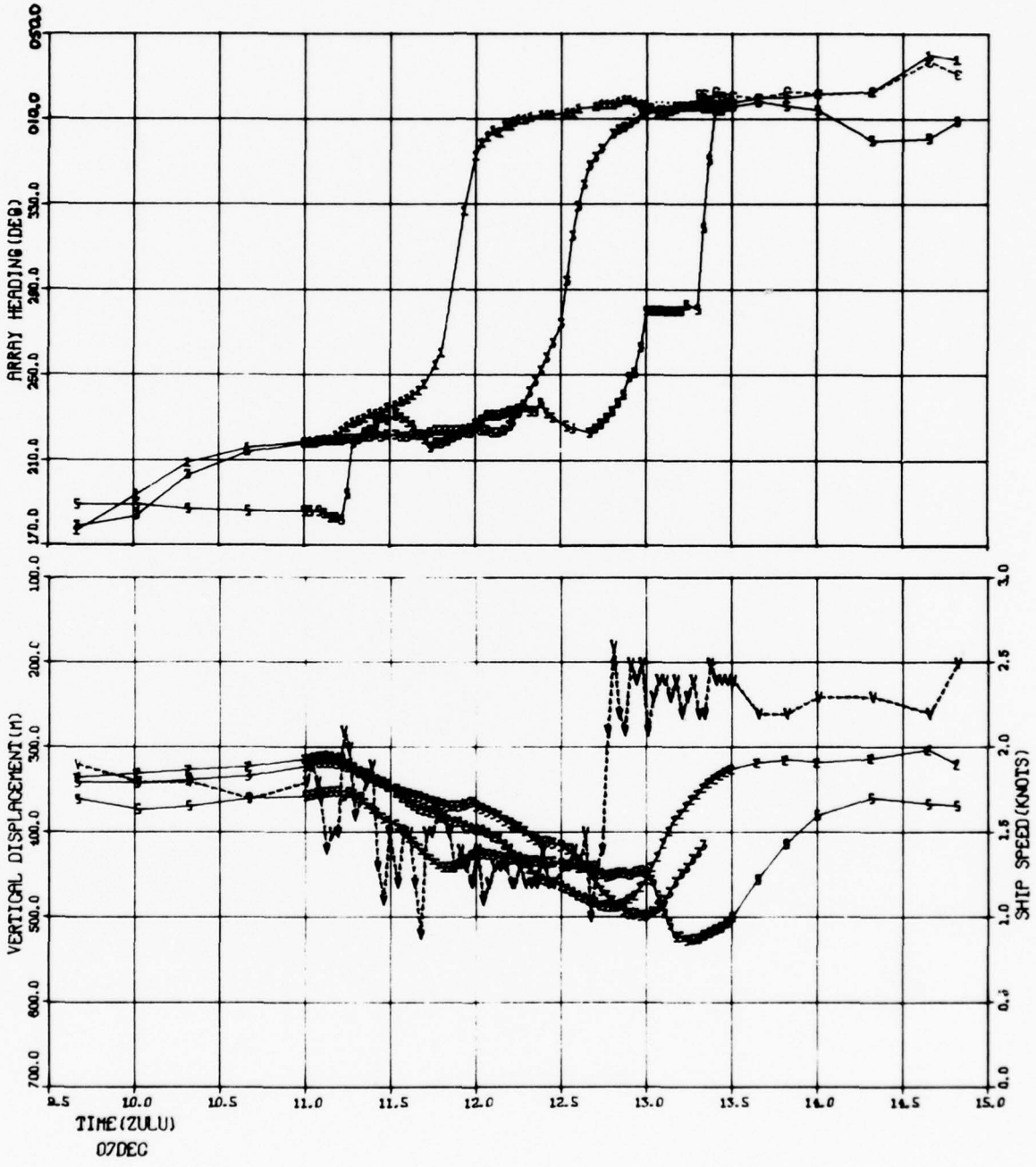
ARRAY HEADING (DEG)
170.0
210.0
250.0
290.0
330.0
010.0
050.0
VERTICAL DISPLACEMENT (M)
100.0
200.0
300.0
400.0
500.0
600.0
700.0
SHIP SPEED (KNOTS)
0.0
0.5
1.0
1.5
2.0
2.5
3.0
9.5
10.0
10.5
11.0
11.5
12.0
12.5
13.0
13.5
14.0
14.5
15.0
TIME (ZULU)
07DEC

TRACK B2 -L26

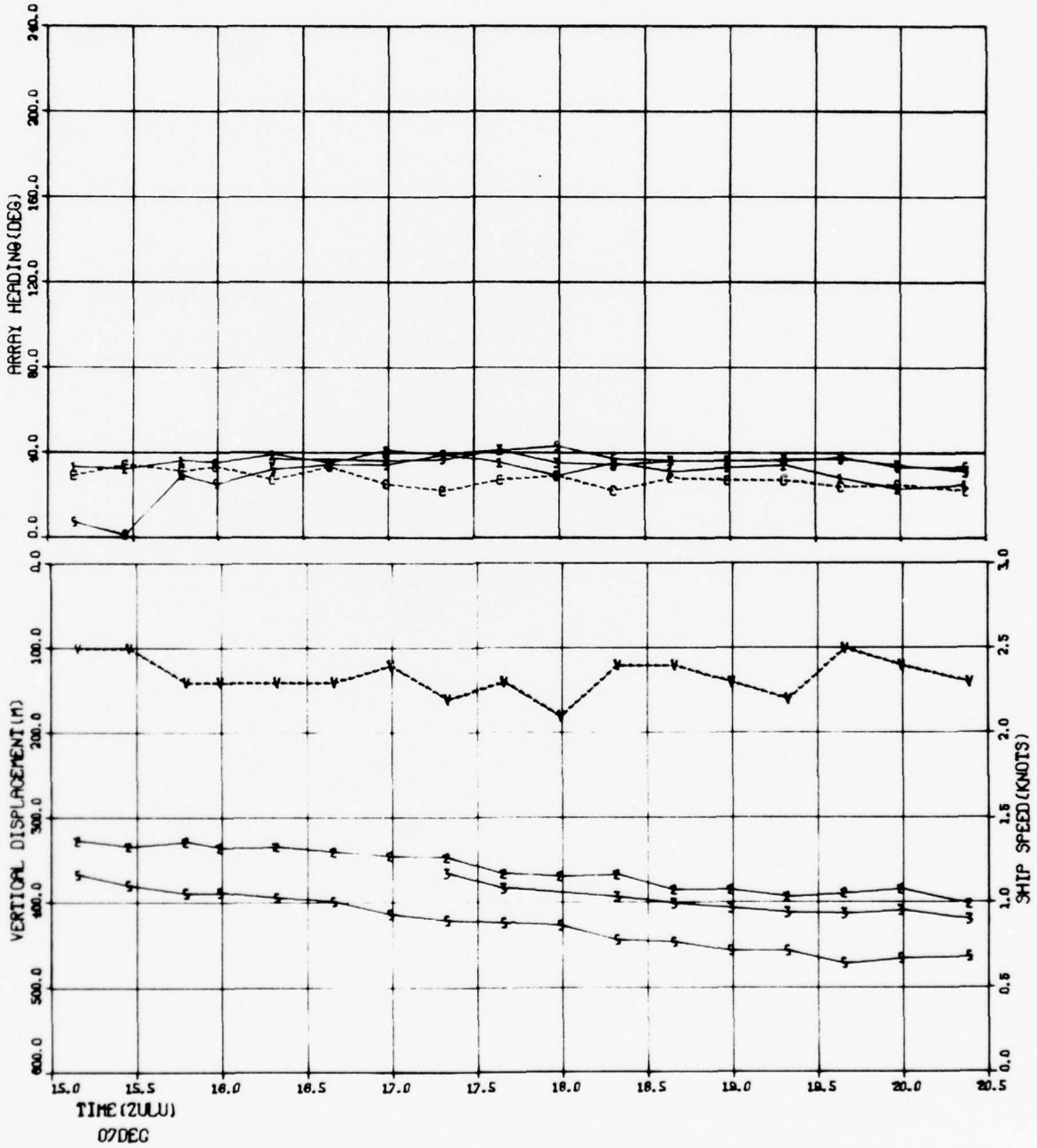
ARRAY HEADING(DEG)
0.0
40.0
80.0
120.0
160.0
200.0
240.0
VERTICAL DISPLACEMENT(M)
0.0
100.0
200.0
300.0
400.0
500.0
600.0
SHIP SPEED(KNOTS)
0.0
0.5
1.0
1.5
2.0
2.5
3.0
15.0
15.5
16.0
16.5
17.0
17.5
18.0
18.5
19.0
19.5
20.0
20.5
TIME(ZULU)
07DEC

TRACK L26-L27

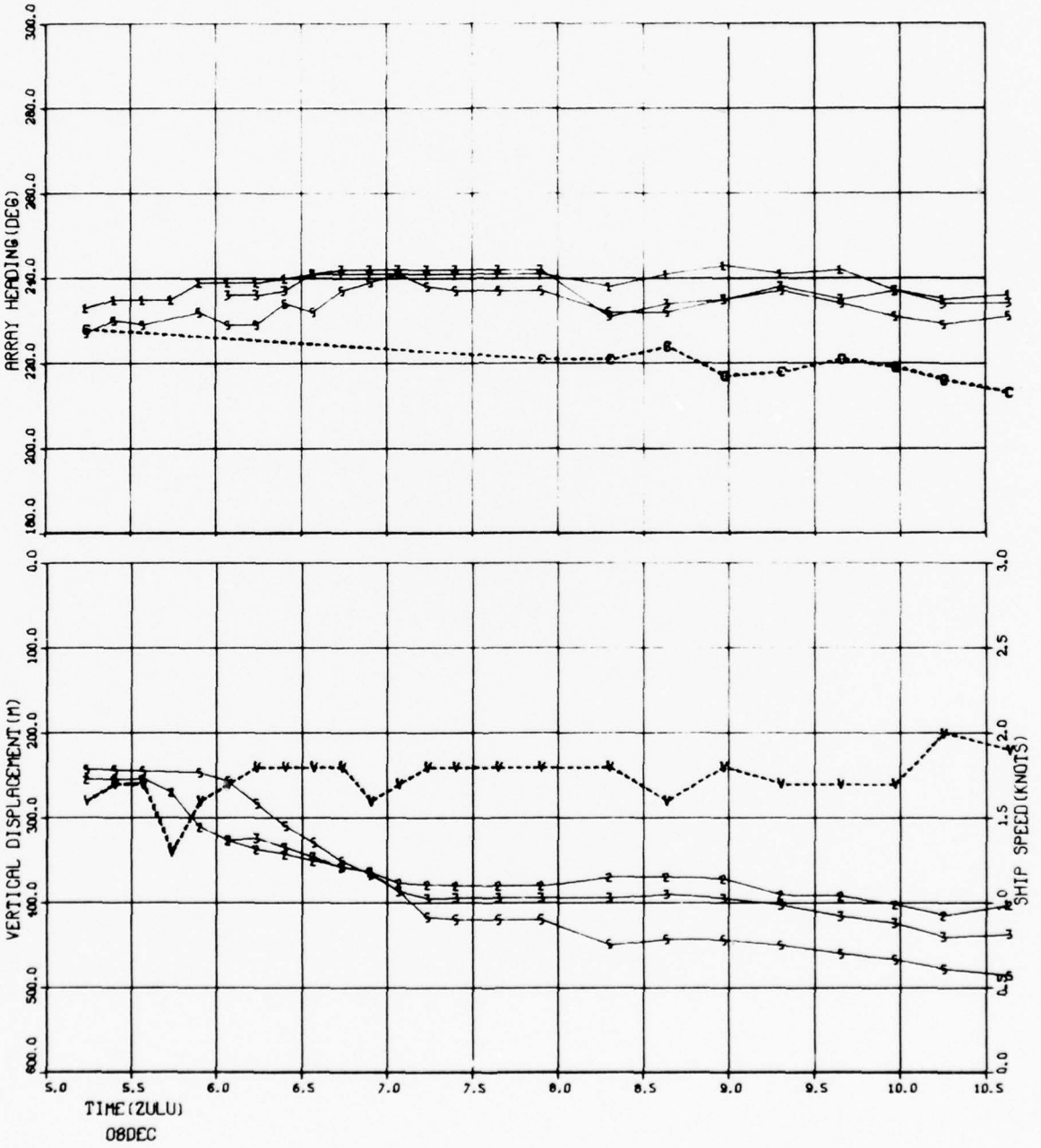

TRACK L26-L27

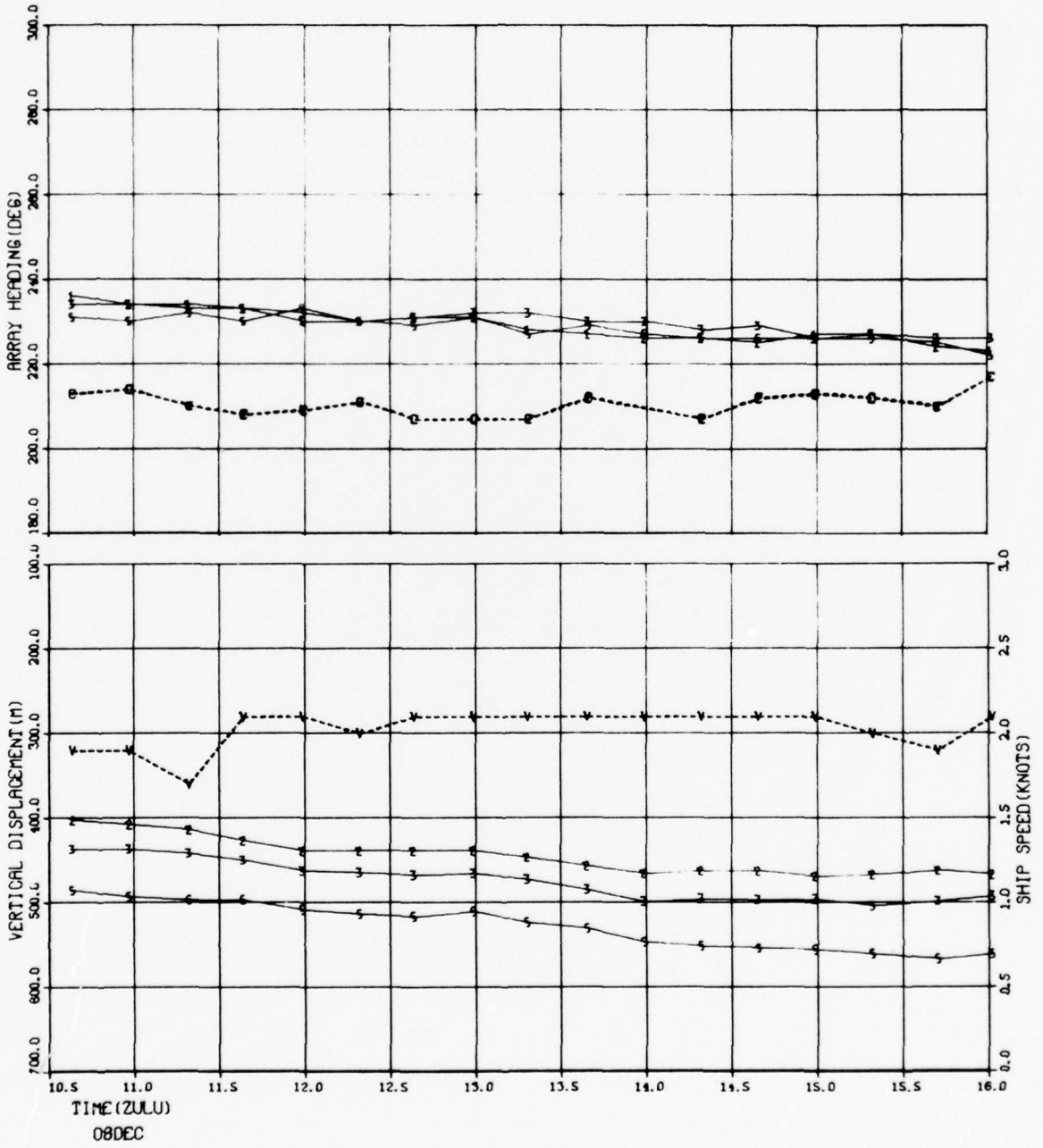

TRACK L26-L27

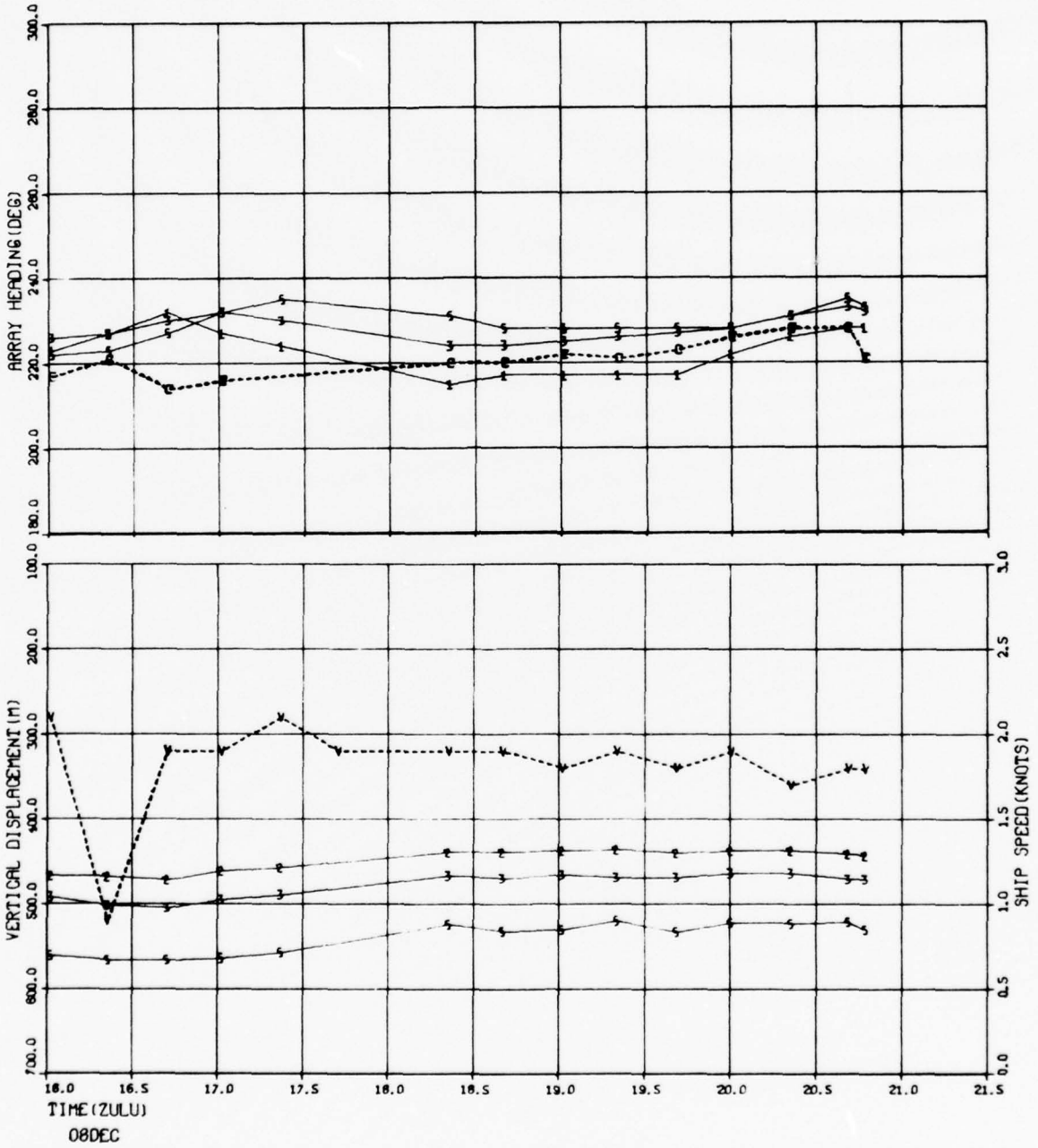

TRACK L26-L27

TRACK L26-L27

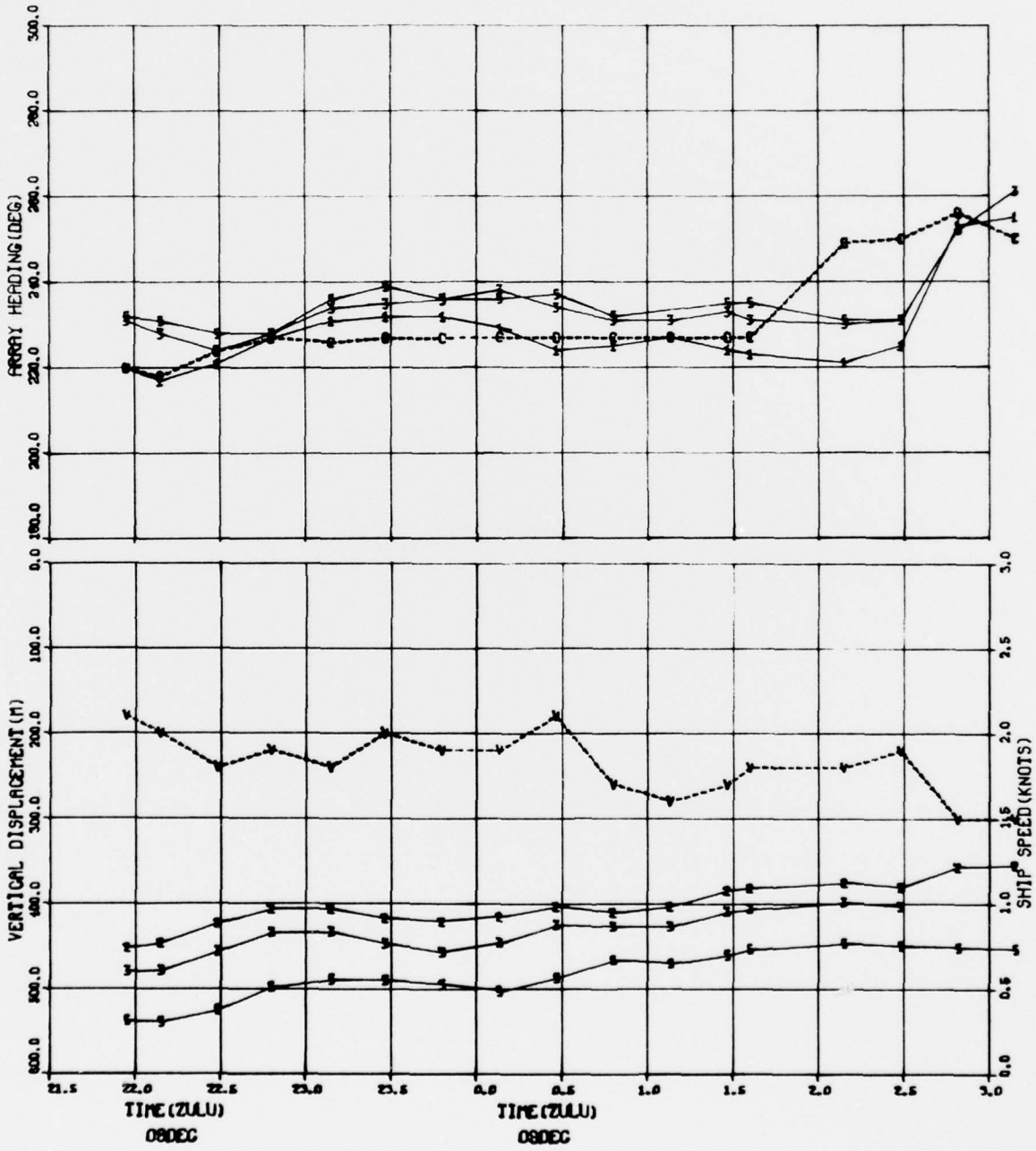

TRACK L26-L27

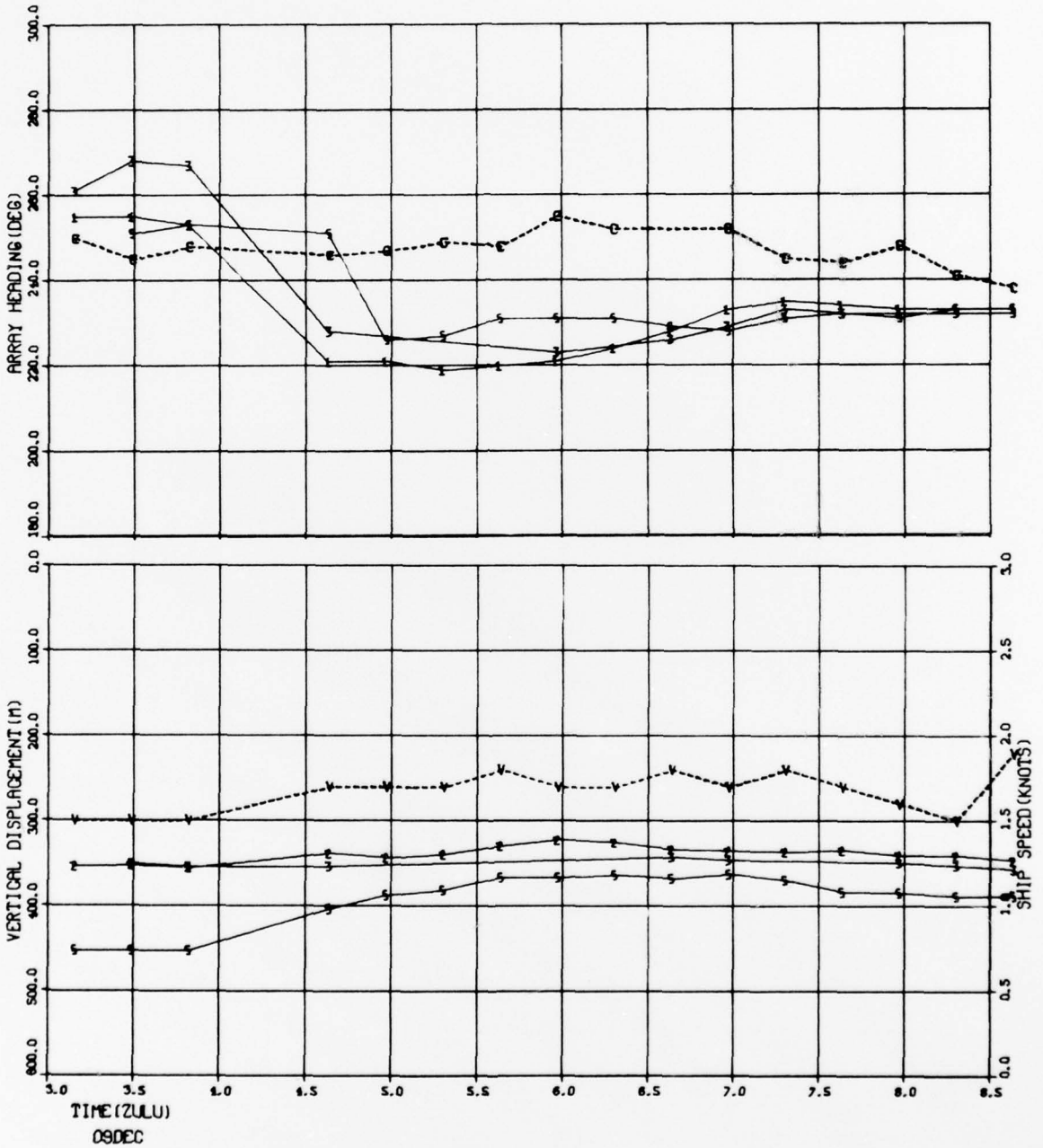

TRACK L26-L27

STATION L27

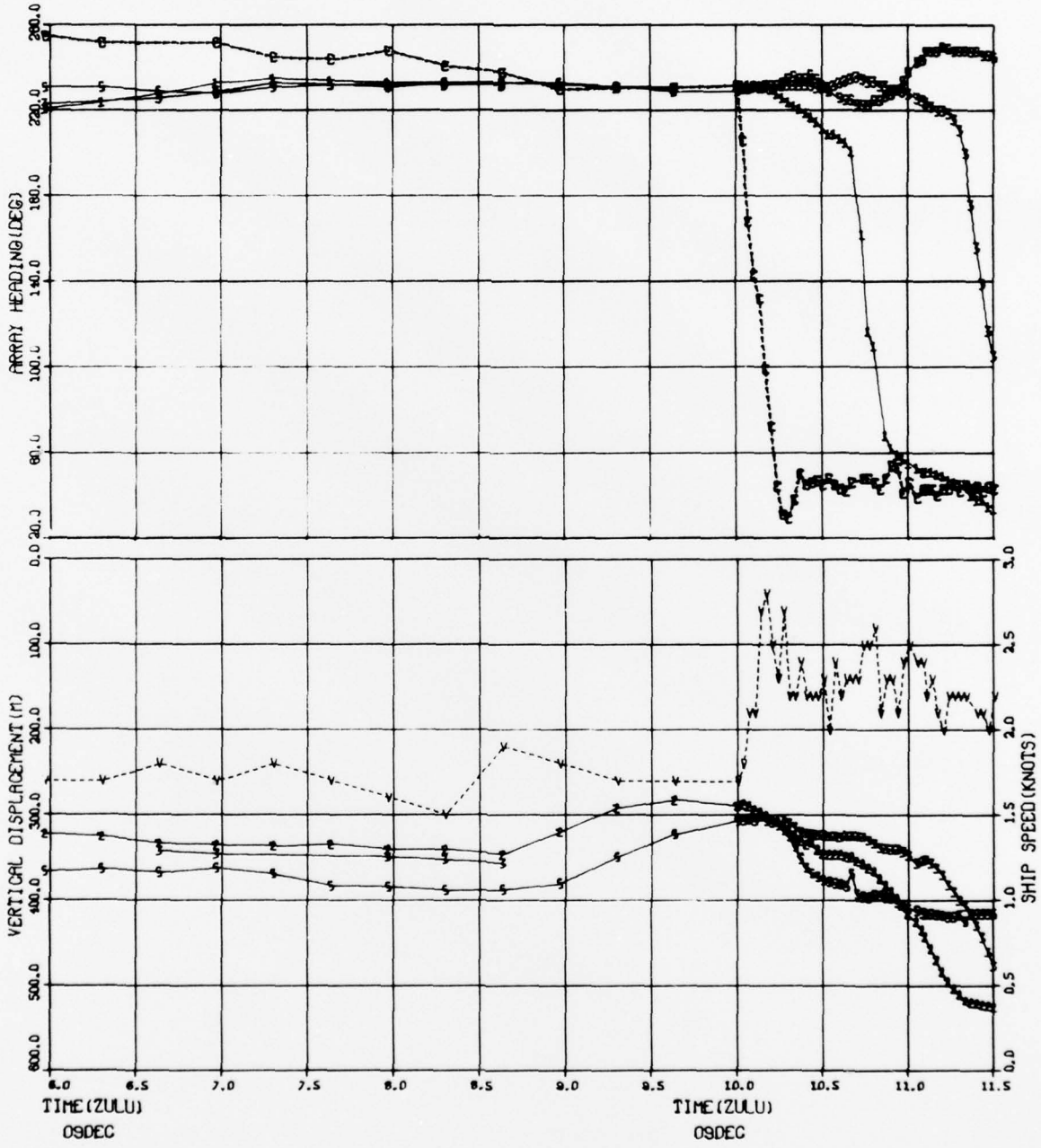

STATION L27 TRACK L27-L28

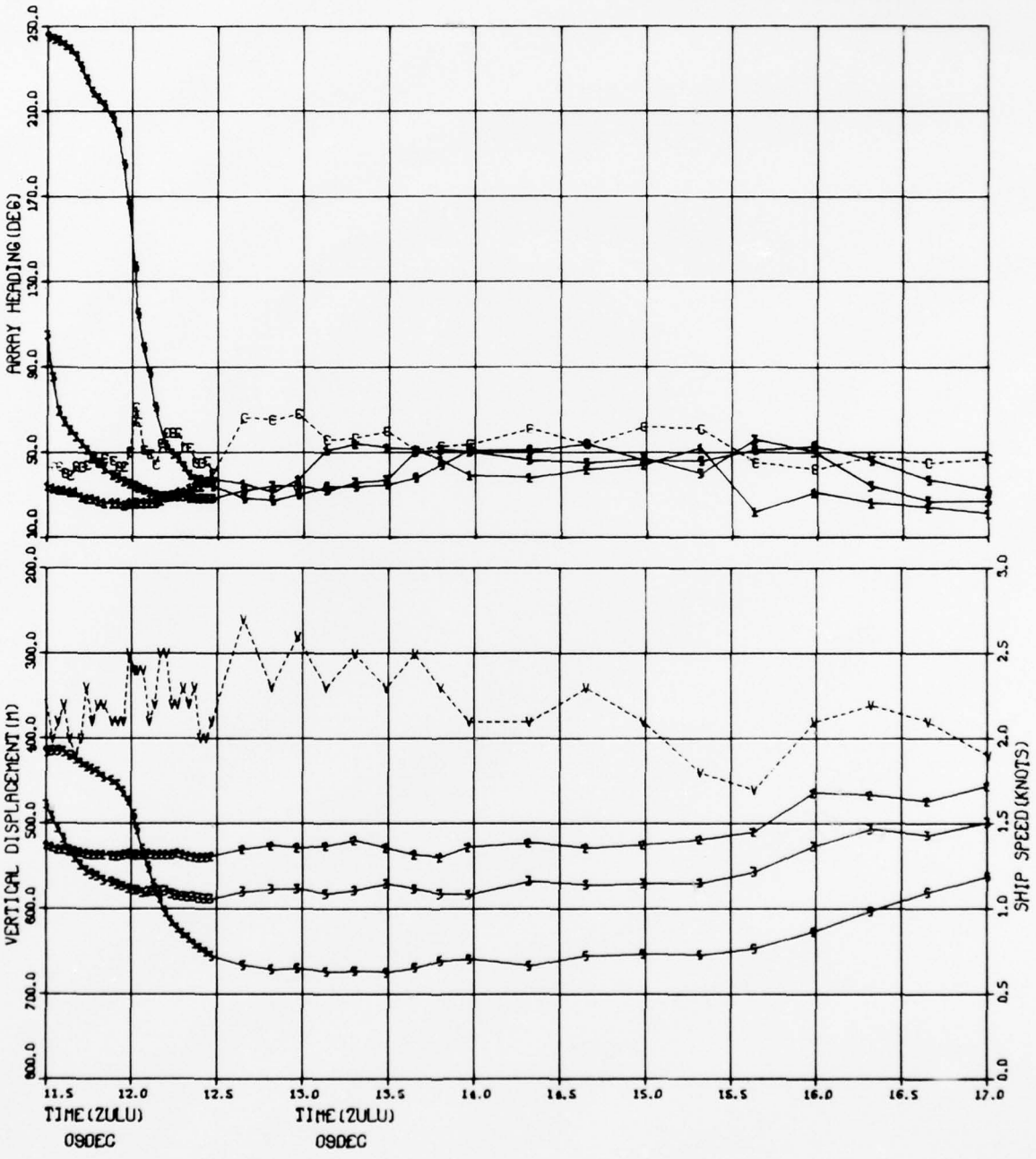

TRACK L27-L28

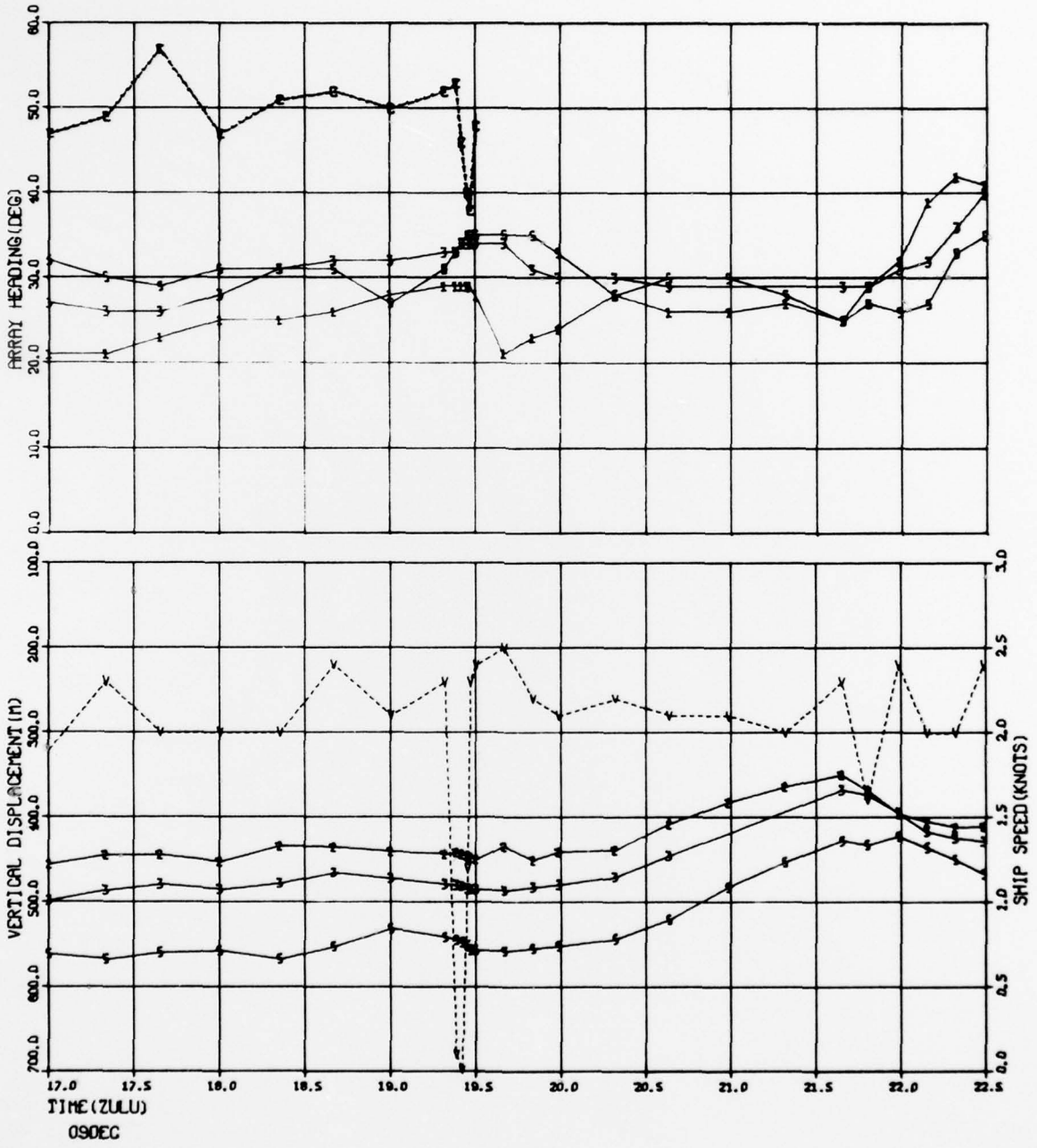

TRACK L27-L28

TRACK L27-L28

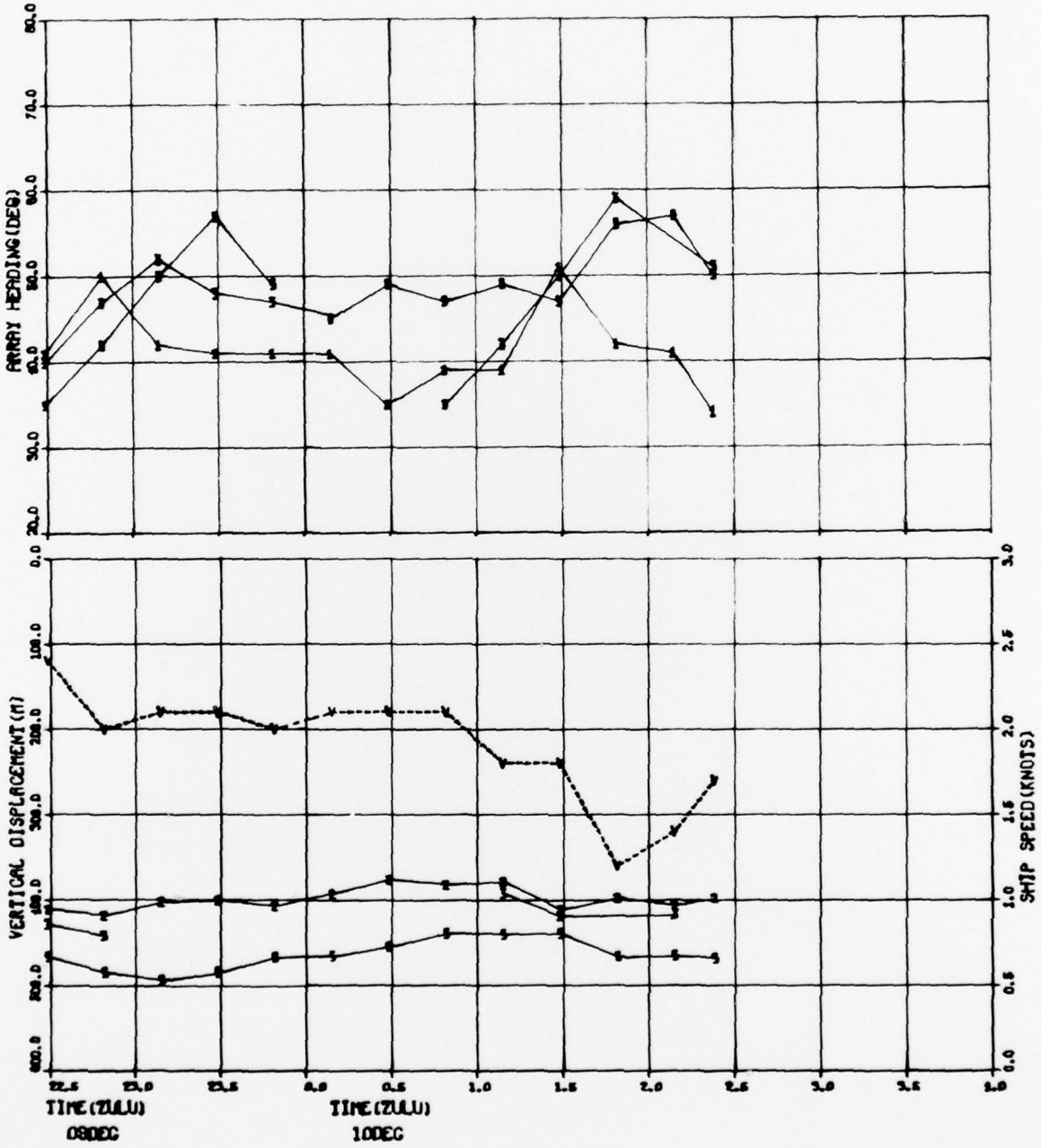

TRACK L27-L28

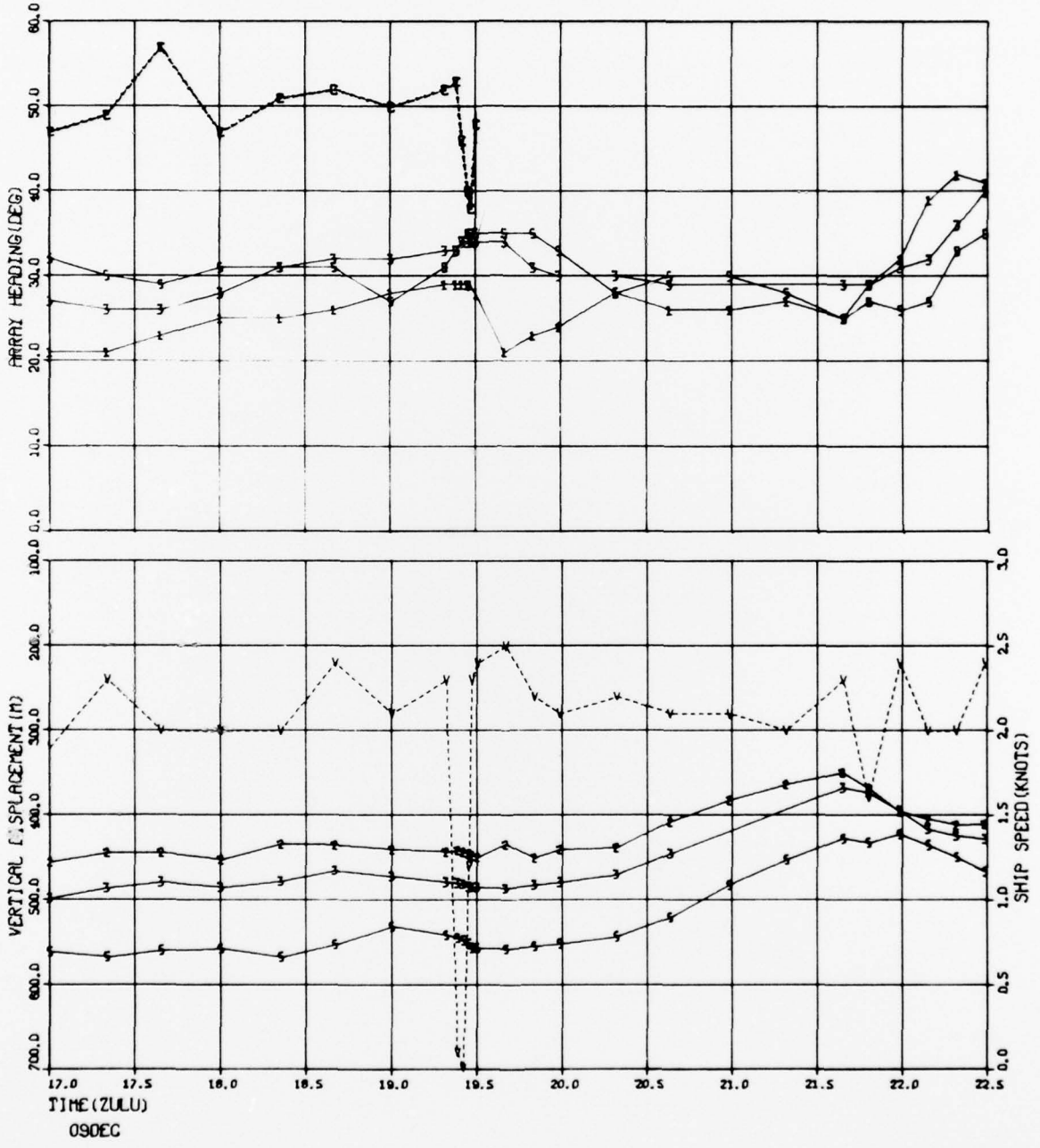

TRACK L27-L28

TRACK L27-L28

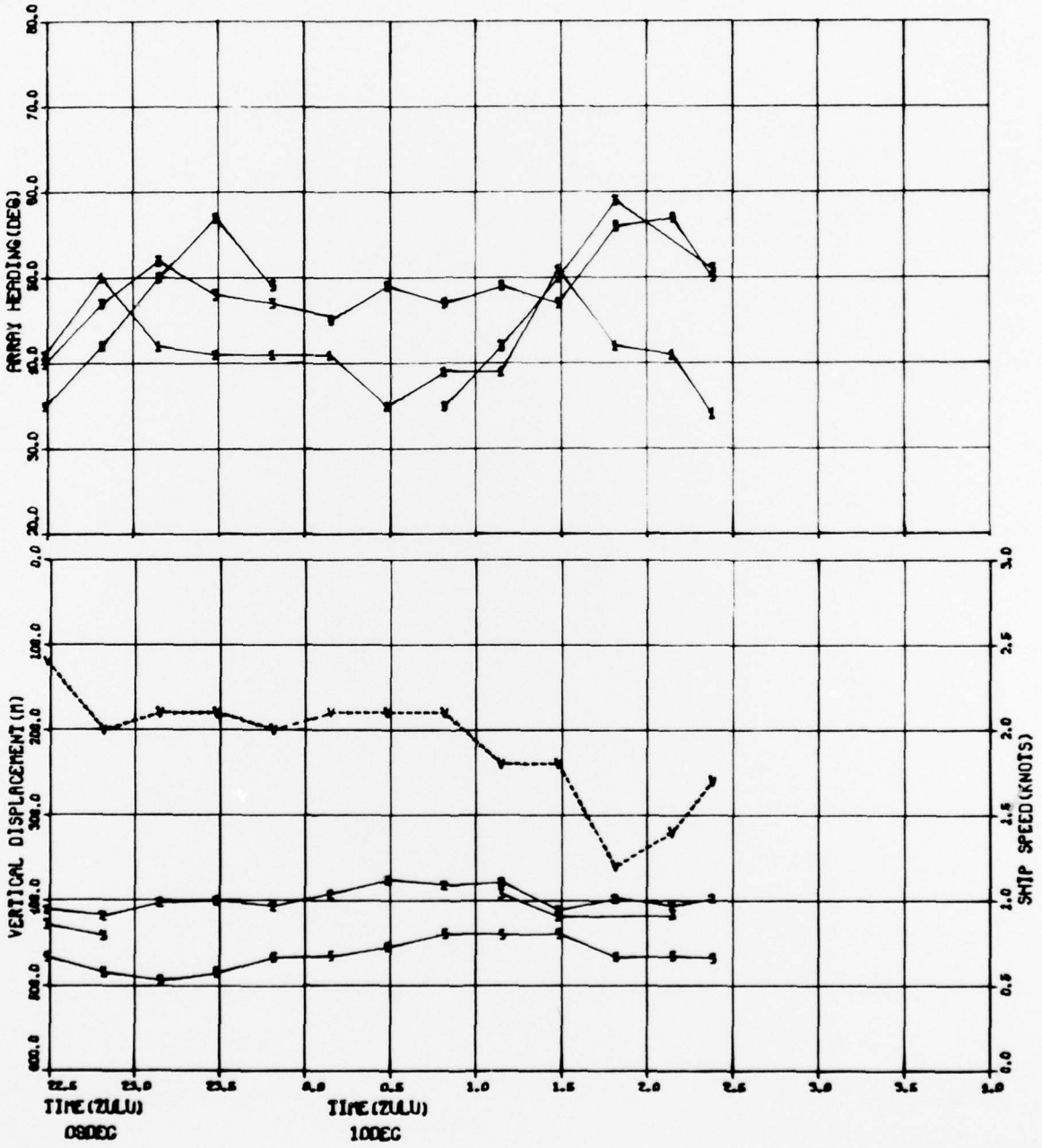

TRACK L27-L28

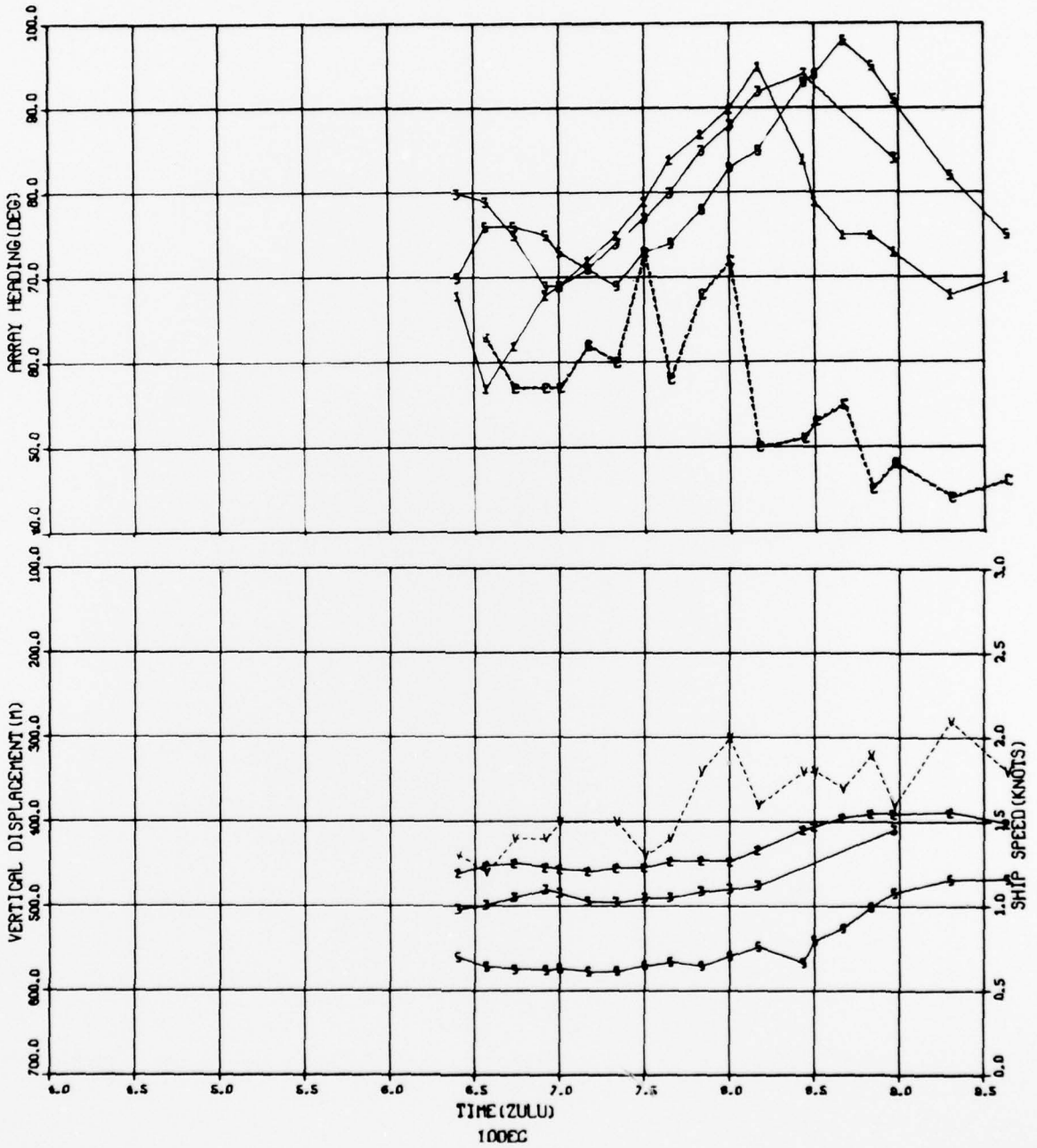

TRACK L27-L28

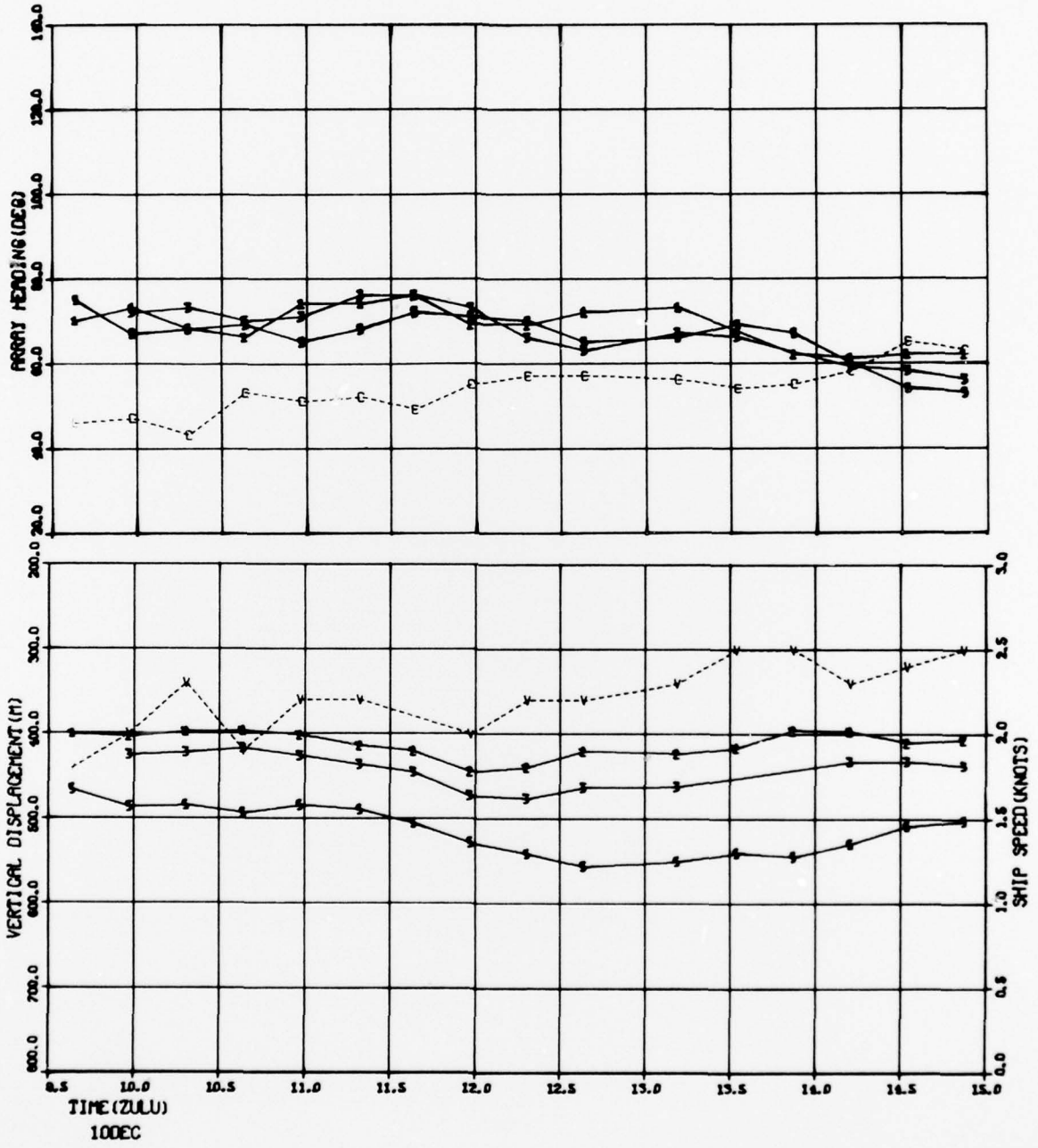

TRACK L27-L28

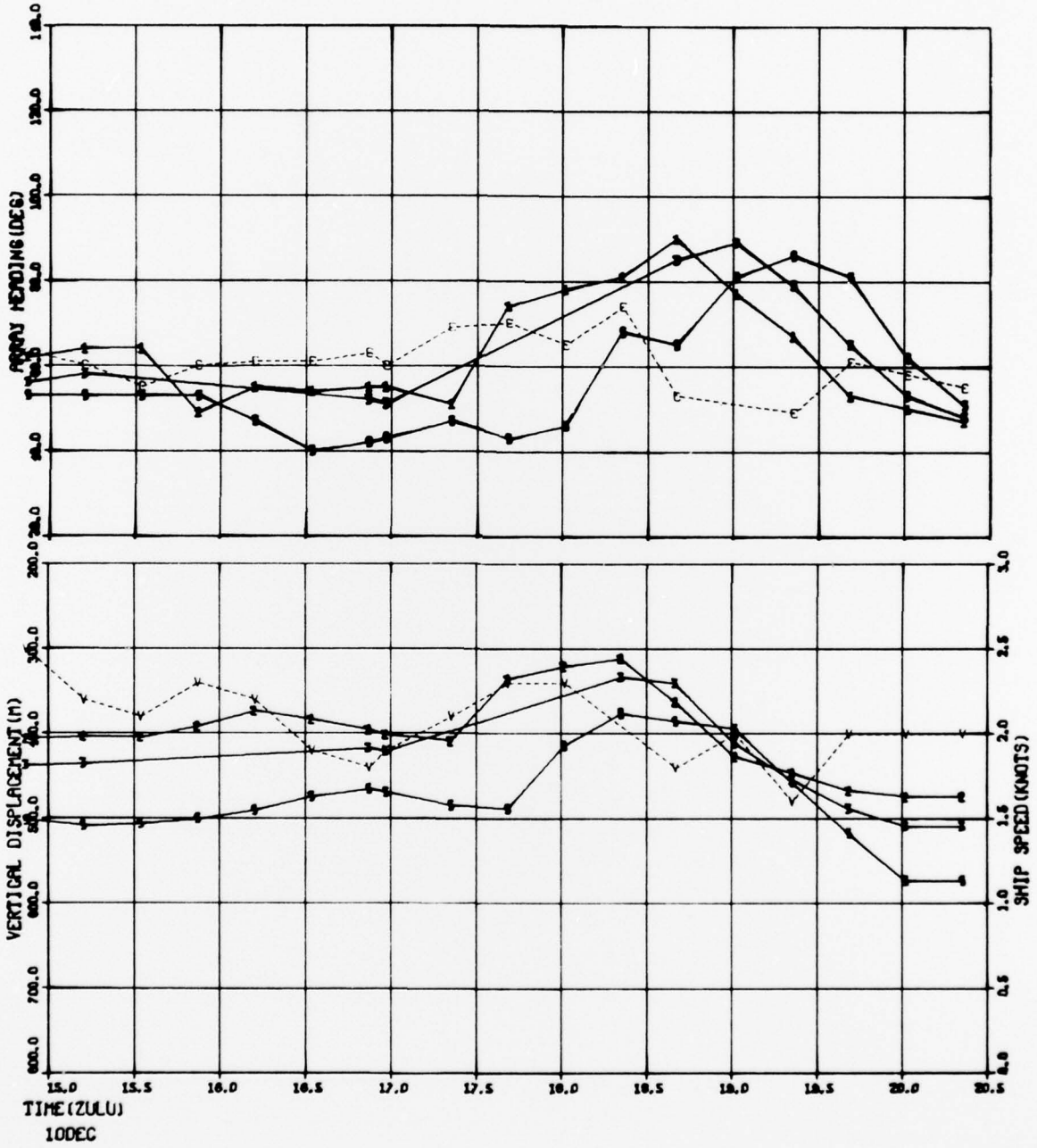

TRACK L27-L28

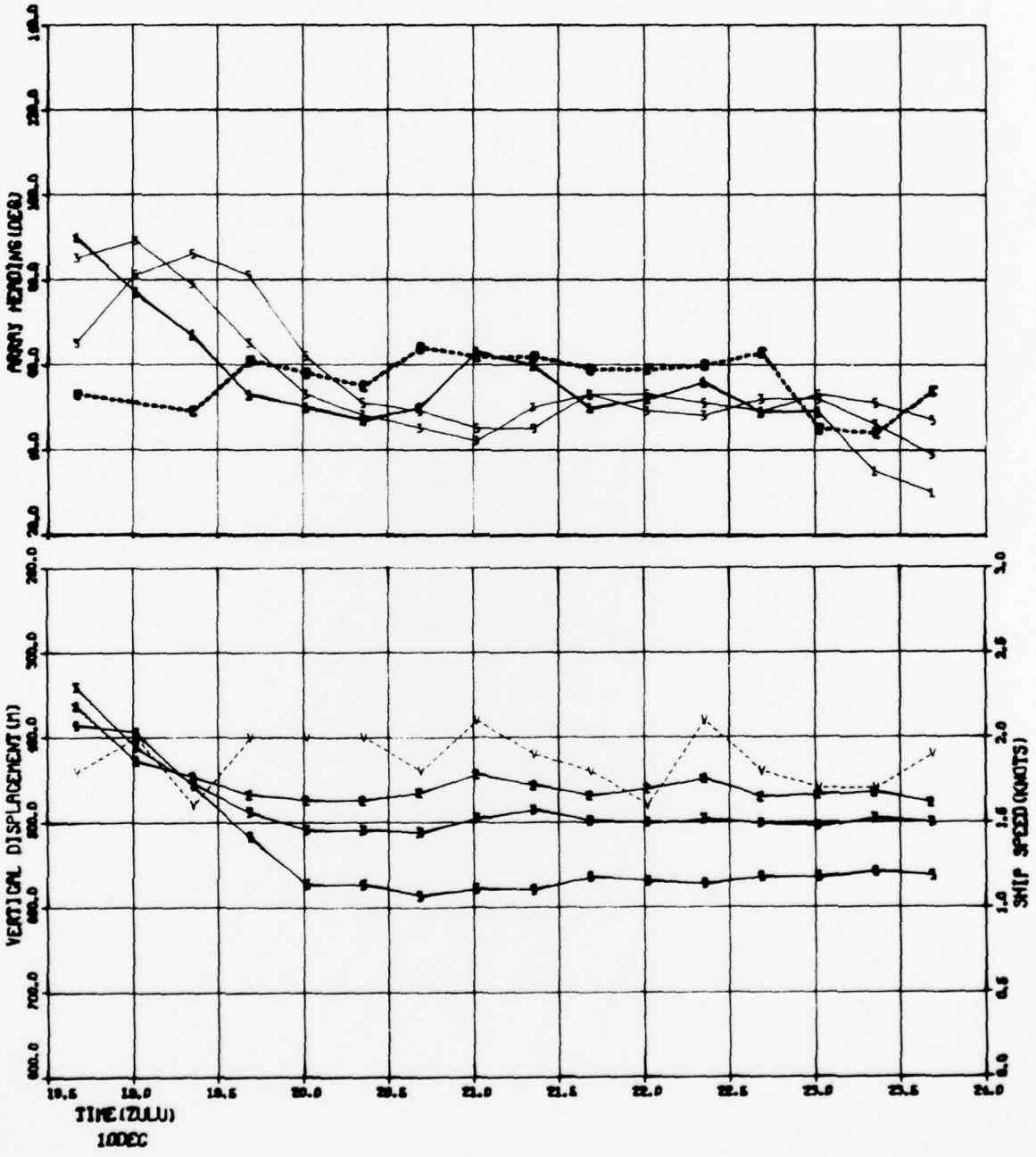

TRACK L27-L28 STATION L28

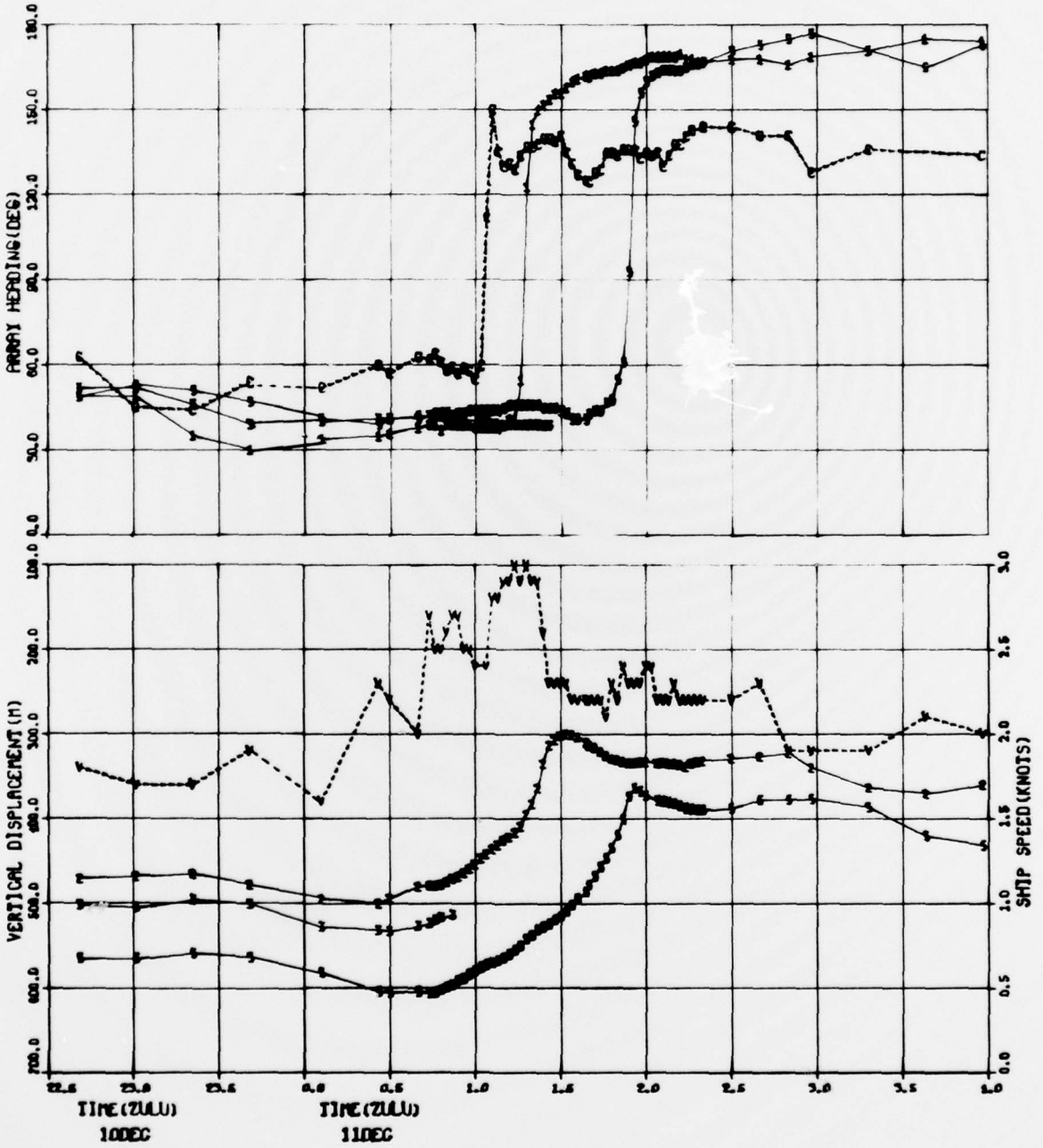

TRACK L28-L29

STATION L29

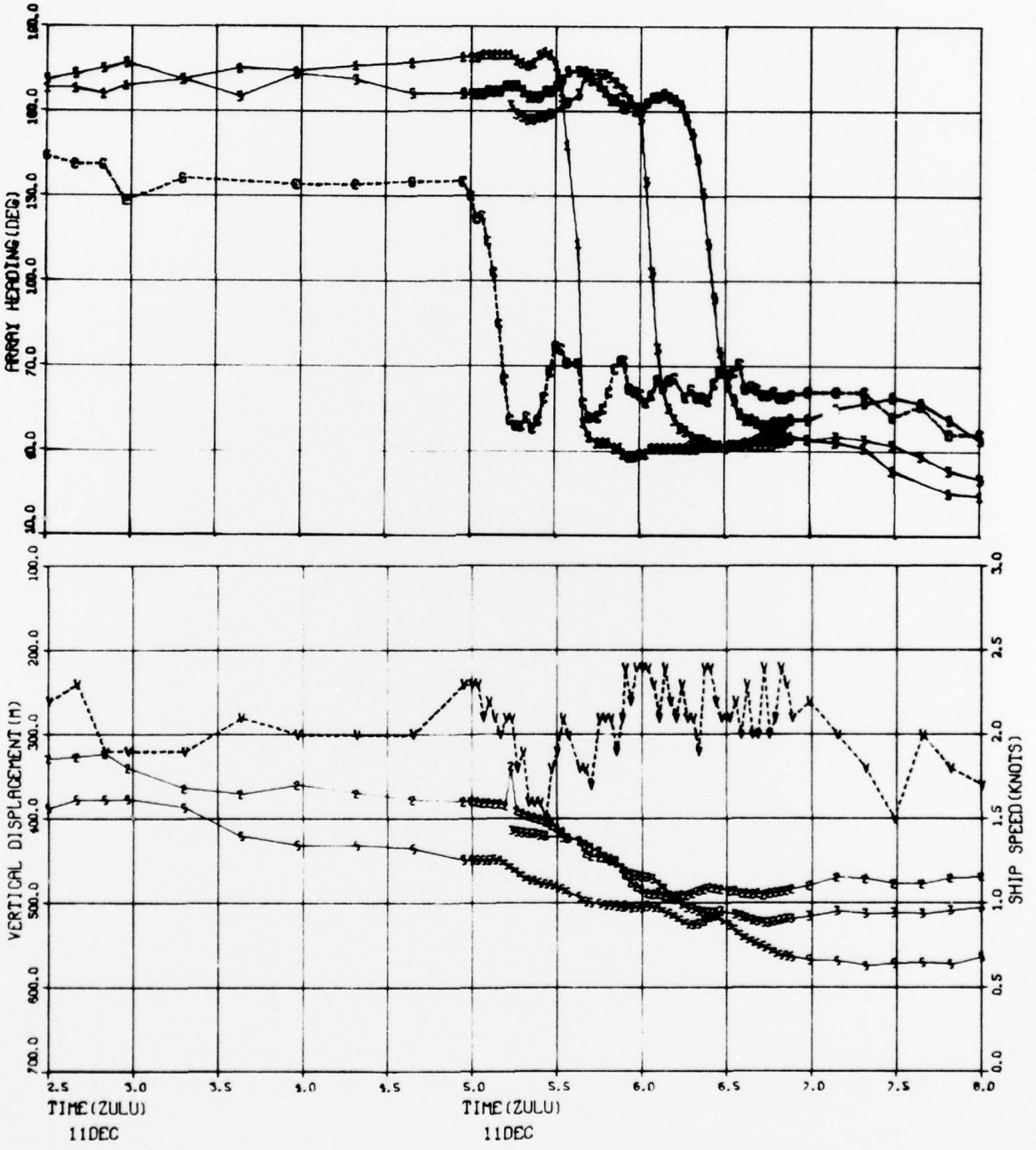

TRACK L29-L30